PHILOSOPHICAL TRANSACTIONS OF THE ROYAL SOCIETY A MATHEMATICAL, PHYSICAL & ENGINEERING SCIENCES

The Development of Travelling Waves in Quadratic and Cubic Autocatalysis with Unequal Diffusion Rates. II. An Initial-Value Problem with an Immobilized or Nearly Immobilized Autocatalyst

J. Billingham and D. J. Needham

Phil. Trans. R. Soc. Lond. A 1991 **336**, 497-539
doi: 10.1098/rsta.1991.0098

The development of travelling waves in quadratic and cubic autocatalysis with unequal diffusion rates. II. An initial-value problem with an immobilized or nearly immobilized autocatalyst

By J. Billingham† and D. J. Needham

School of Mathematics, University of East Anglia, Norwich NR4 7TJ, U.K.

Contents

We study the isothermal autocatalytic reaction schemes, $A + B \rightarrow 2B$ (quadratic autocatalysis), and $A + 2B \rightarrow 3B$ (cubic autocatalysis), where A is a reactant and B is an autocatalyst. We consider the situation when a quantity of B is introduced locally into a uniform expanse of A, in one-dimensional slab geometry. In addition, we allow the chemical species A and B to have unequal diffusion rates D_A and D_B, respectively, and study the two closely related cases, $(D_B/D_A) = 0$ and $0 < (D_B/D_A) \ll 1$. When $(D_B/D_A) = 0$ a spike forms in the concentration of B, which grows indefinitely, and we can obtain both large and small time asymptotic solutions. For $0 < (D_B/D_A) \ll 1$ there is a long induction period during which a large spike forms in the concentration of B, before a minimum speed travelling wave is generated. We can relate the results for case $(D_B/D_A) = 0$ to the solution when $0 < (D_B/D_A) \ll 1$ to obtain detailed information about its behaviour.

† Present address: Schlumberger Cambridge Research, PO Box 153, Cambridge CB3 0HG, U.K.

Phil. Trans. R. Soc. Lond. A (1991) **336**, 497–539
Printed in Great Britain

1. Introduction

In part I of this series of papers (Billingham & Needham 1991*a*, henceforth referred to as BN) we studied two model, isothermal, autocatalytic chemical reaction schemes. The first scheme was based on the quadratic autocatalytic step

$$\mathrm{A}+\mathrm{B}\rightarrow 2\mathrm{B}, \quad \text{rate} \quad k_1 ab, \tag{1}$$

whilst the second scheme was based on the cubic autocatalytic step

$$\mathrm{A}+2\mathrm{B}\rightarrow 3\mathrm{B}, \quad \text{rate} \quad k_2 ab^2. \tag{2}$$

Here a and b are the concentrations of the reactant, A, and the autocatalyst, B, respectively, and k_1 and k_2 are reaction rate constants. The chemical viability of the reaction steps (1) and (2) was discussed in BN, in particular, see Sel'kov (1968), Gray *et al.* (1984), Merkin *et al.* (1985) and Aris *et al.* (1988). In BN we considered the travelling waves that may be generated when a quantity of the autocatalyst, B, is introduced locally into an expanse of the reactant, A, which is initially at a uniform concentration. In the present paper we continue our analysis of this initial-value problem. To simplify the analysis we restrict attention to the case of one-dimensional slab geometry with the coordinate $\bar{x}$ measuring distance.

The equations which govern the reaction and diffusion of the species A and B under reaction schemes (1) and (2) are

$$\partial a/\partial \bar{t} = D_{\mathrm{A}}\,\partial^2 a/\partial \bar{x}^2 - k_n\, ab^n, \quad \partial b/\partial \bar{t} = D_{\mathrm{B}}\,\partial^2 b/\partial \bar{x}^2 + k_n\, ab^n. \tag{3a, b}$$

Here $\bar{t}$ is time and D_{A} and D_{B} are the constant diffusion rates of the reactant, A, and the autocatalyst, B, respectively. Under quadratic autocatalysis $n = 1$, while for cubic autocatalysis $n = 2$. The initial conditions are

$$a(\bar{x}, 0) = a_0, \quad b(\bar{x}, 0) = b_0\, g(\bar{x}), \quad |\bar{x}| < \infty, \tag{4a}$$

where a_0 and b_0 are the positive, constant, initial concentration of A and maximum initial concentration of B respectively. We now restrict attention to situations where the initial input of B has compact support, so that $g(\bar{x})$ is a given, non-negative function of $\bar{x}$ with a maximum value of unity and $g(\bar{x}) = 0$ for $|\bar{x}| > l$, where l is a positive, constant length. In addition, we consider the function $g(\bar{x})$ to be analytic in $|\bar{x}| \leqslant l$. The boundary conditions to be statisfied by the concentrations a and b are

$$a(\bar{x}, \bar{t}) \rightarrow a_0, \quad b(\bar{x}, \bar{t}) \rightarrow 0 \quad \text{as} \quad |\bar{x}| \rightarrow \infty, \quad \bar{t} \geqslant 0. \tag{4b}$$

For the purpose of this paper it is also convenient to consider $g(\bar{x})$ to be symmetric about the point $\bar{x} = 0$. The problem can now be reduced to the domain $\bar{x} \geqslant 0$ with a symmetry condition at $\bar{x} = 0$. After making this additional assumption, which is not at all restrictive, the initial and boundary conditions (4*a*, *b*) become

$$a(\bar{x}, 0) = a_0, \quad b(\bar{x}, 0) = b_0\, g(\bar{x}), \quad \bar{x} \geqslant 0, \tag{5a}$$

$$\partial a/\partial \bar{x}\,(0, \bar{t}) = \partial b/\partial \bar{x}\,(0, \bar{t}) = 0, \quad \bar{t} \geqslant 0, \tag{5b}$$

$$a(\bar{x}, \bar{t}) \rightarrow a_0, \quad b(\bar{x}, \bar{t}) \rightarrow 0 \quad \text{as} \quad \bar{x} \rightarrow \infty, \quad \bar{t} \geqslant 0. \tag{5c}$$

The initial-value problem given by equations (3*a*, *b*) together with initial and boundary conditions (5) is also appropriate to model the situation where the reaction proceeds on the domain $\bar{x} \geqslant 0$ with an impermeable wall positioned at $\bar{x} = 0$. The initial input of the autocatalyst, B, is then confined to the region $0 \leqslant \bar{x} \leqslant l$.

It is convenient to introduce dimensionless variables as

$$\alpha = a/a_0, \quad \beta = b/b_0, \quad t = k_n a_0^n \bar{t}, \quad x = (k_n a_0^n/D_A)^{\frac{1}{2}} \bar{x}, \tag{6}$$

in terms of which equations (3*a*, *b*) together with initial and boundary conditions (5) become

$$\partial\alpha/\partial t = \partial^2\alpha/\partial x^2 - \alpha\beta^n, \quad \partial\beta/\partial t = D\,\partial^2\beta/\partial x^2 + \alpha\beta^n, \tag{7a, b}$$

$$\alpha(x, 0) = 1, \quad \beta(x, 0) = \beta_0 g(x), \quad x \geqslant 0, \tag{8a}$$

$$(\partial\alpha/\partial x)(0, t) = (\partial\beta/\partial x)(0, t) = 0, \quad t \geqslant 0, \tag{8b}$$

$$\alpha(x, t) \to 1, \quad \beta(x, t) \to 0 \quad \text{as} \quad x \to \infty, \quad t \geqslant 0. \tag{8c}$$

The parameter $\lambda = (k_n a_0^n/D_A)^{\frac{1}{2}} l$ provides a dimensionless measure of the width of the initial input of the autocatalyst, since $g(x) = 0$ for $x \geqslant \lambda$. The dimensionless parameter $\beta_0 = b_0/a_0$ is a measure of the maximum concentration of the initial input of B, while the dimensionless parameter $D = D_B/D_A$ measures the rate of diffusion of the autocatalyst, B, relative to that of the reactant, A. In addition, with $g(x)$ analytic in $0 \leqslant x \leqslant \lambda$ we have that

$$g(x) \sim g_\lambda(\lambda - x)^P \quad \text{as} \quad x \to \lambda^-, \tag{8d}$$

for some positive constant g_λ and $P \in \mathbb{N}$.

In this paper we study two special cases: $0 < D \ll 1$, which models the reaction when the autocatalyst diffuses much more slowly than the reactant; and $D = 0$, which models the reaction when the autocatalyst cannot diffuse. These two cases can occur in enzyme reactions. The first situation, $0 < D \ll 1$, arises when the reaction involves large enzyme molecules and much smaller substrate molecules so that the enzyme diffuses much more slowly than the substrate. The second situation occurs when the enzyme is immobilized in a gel or membrane. Equations (7) also arise in epidemiology, where α represents the number density of healthy individuals and β the number density of infected individuals (see, for example, Bailey 1975). Infected individuals are generally less mobile than healthy individuals, a situation which can lead to either of the two cases $0 < D \ll 1$ or $D = 0$. With $D = 1$, the initial-value problem (7, 8) has been studied by Gray *et al.* (1990), and with modifications to include termination steps by Merkin *et al.* (1989) and Merkin & Needham (1990).

In BN we studied the permanent form travelling wave solutions of equations (7*a*, *b*). These are non-trivial, non-negative solutions that depend only on the single variable $z \equiv x - vt$, where v is the constant propagation speed, and satisfy the conditions $\alpha \to 1$, $\beta \to 0$ as $z \to \infty$ and $\alpha \to 0$, $\beta \to 1$ as $z \to -\infty$. We found that such a solution exists for each $v \geqslant v_n^*(D)$, where $v_n^*(D)$ is a non-negative, monotone increasing function of D that represents the minimum propagation speed. We also demonstrated that

$$v_1^*(D) \equiv 2\sqrt{D} \quad \text{for all} \quad D \geqslant 0, \tag{9a}$$

$$v_2^*(D) \sim \tilde{v}_2^* D \quad \text{for} \quad 0 \leqslant D \ll 1, \tag{9b}$$

where $\tilde{v}_2^* = 1.219\ldots$. In a later paper (Billingham & Needham 1991*b*), we will show that a travelling wave, which propagates out of the initial-reaction region with the minimum speed $v_n^*(D)$, is formed in the initial-value problem (7), (8) when $g(x)$ has compact support and $D > 0$. However, when $D = 0$ the autocatalyst, B, cannot diffuse into the region $x \geqslant \lambda$, so travelling waves cannot develop. This is consistent with the result, $v_1^*(0) = v_2^*(0) = 0$.

In this paper we begin by studying numerical solutions of the initial-value problem (7), (8) under both quadratic autocatalysis, $n = 1$, and cubic autocatalysis, $n = 2$. When $0 < D \ll 1$ we find that there is a long induction period before the formation of a minimum speed travelling wave. During this induction period, well-defined transient features are observed in the numerical solutions, as described in §2.

We analyse these transient features in the solutions of the initial-value problem (7), (8), when $0 < D \ll 1$, by examining in detail the initial-value problem when $D = 0$. This problem has applications in its own right, as mentioned earlier. With $D = 0$, a simple integration of equation (7*b*), together with an application of condition (8*a*), leads to

$$\beta(x,t) = \beta_0 g(x) \exp\left\{\int_0^t \alpha(x,\tau)\,\mathrm{d}\tau\right\}, \quad n = 1, \tag{10a}$$

$$\beta(x,t) = \beta_0 g(x)\left\{1-\beta_0 g(x)\int_0^t \alpha(x,\tau)\,\mathrm{d}\tau\right\}^{-1}, \quad n = 2. \tag{10b}$$

Since $g(x) = 0$ for $x > \lambda$, we deduce immediately from (10) that $\beta(x,t) = 0$ for $x > \lambda$, $t \geqslant 0$. This enables us to reformulate the initial-value problem (7), (8), as $x \geqslant \lambda$, $t \geqslant 0$

$$\partial\alpha_+/\partial t = \partial^2\alpha_+/\partial x^2, \tag{11a}$$

$$\alpha_+(x,0) = 1, \quad \alpha_+(x,t) \to 1 \quad \text{as} \quad x \to \infty; \tag{11b, c}$$

$0 \leqslant x \leqslant \lambda, t \geqslant 0$

$$\partial\alpha_-/\partial t = \partial^2\alpha_-/\partial x^2 - \alpha_-\beta^n, \quad \partial\beta/\partial t = \alpha_-\beta^n, \tag{12a, b}$$

$$\alpha_-(x,0) = 1, \quad \beta(x,0) = \beta_0 g(x), \quad (\partial\alpha_-/\partial x)(0,t) = 0 \tag{12c, d}$$

together with the connection conditions

$$\alpha_+(\lambda,t) = \alpha_-(\lambda,t), \quad (\partial\alpha_+/\partial x)(\lambda,t) = (\partial\alpha_-/\partial x)(\lambda,t) \quad \text{for} \quad t \geqslant 0. \tag{13a, b}$$

Here we have defined $\alpha_+(x,t)$ and $\alpha_-(x,t)$ so that

$$\alpha(x,t) = \begin{cases} \alpha_+(x,t), & x > \lambda, \\ \alpha_-(x,t), & 0 \leqslant x \leqslant \lambda. \end{cases} \tag{14a, b}$$

In §2 we consider numerical solutions of the initial-value problem (11)–(13). An examination of these numerical solutions suggests that it is possible to develop asymptotic solutions of the initial-value problem (11)–(13) for $0 \leqslant t \ll 1$ and $t \gg 1$. The asymptotic behaviour for $t \gg 1$ is of primary interest and we consider this in §3, whilst the details of the development for $t \ll 1$ may be found in Billingham (1991).

The solution of the initial-value problem (11)–(13) can be regarded as the first approximation to the solution of the initial-value problem (7), (8) with $0 < D \ll 1$. In §4 we use our knowledge of the asymptotic solution for $t \gg 1$ when $D = 0$, which enables us to construct asymptotic solutions for (7), (8) as $D \to 0$, valid up to $t = O(D^{-\frac{1}{2}})$, for $n = 1$, and $t = O((\ln D)^2)$ for $n = 2$. Finally, we describe the complete asymptotic structure of the solution for all $t \geqslant 0$, $x \geqslant 0$ of the initial-value problem (7), (8) as $D \to 0$ under quadratic autocatalysis, $n = 1$. This consists of ten asymptotic regions, and we determine the leading order solution in all but one of these. In particular, we find that a propagating wave front is always generated in the long time

and that the leading order problem in the region ahead of the wave front is a nonlinear eigenvalue problem for v, the travelling wave propagation speed, which determines v uniquely as the minimum propagation speed, $v = 2\sqrt{D}$. For cubic autocatalysis, $n = 2$, it is not possible to construct the full asymptotic solution for all $t \geqslant 0$ as $D \to 0$. However, by determining upper and lower bounds on the asymptotic solution in the neighbourhood of the point $x = \lambda$, we can gain a full understanding of the development of the solution.

2. Numerical solution of the initial-value problem

In this section we obtain numerical solutions of the initial-value problem (7), (8). For the purpose of numerical integration, we take the functional form of the initial input of the autocatalyst to be

$$g(x) = \{1-(x/\lambda)^2\}^p \quad \text{for} \quad 0 \leqslant x \leqslant \lambda, \tag{15}$$

with $p \in \mathbb{N}$. The function $g(x)$ is thus of $0\{(\lambda - x)^p\}$ as $x \to \lambda^-$. The numerical solutions were obtained using a modified Crank–Nicolson technique, and error checks were performed at each time step. The details of the numerical method are not given here, but may be found in Billingham (1991). To obtain additional information about the solution, at each time step we calculate the functions $\beta_{\max}$ and $P(t)$ defined by

$$\beta_{\max}(t) = \sup_{0 \leqslant x \leqslant L} \{\beta(x,t)\}, \tag{16a}$$

$$|\beta(P(t),t) - \tfrac{1}{2}| = \inf_{0 \leqslant x \leqslant L} \{|\beta(x,t) - \tfrac{1}{2}|\}, \tag{16b}$$

where L is the extent of the large, but finite, domain in x over which the numerical integrations were performed. The function $\beta_{\max}(t)$ is the maximum value of β at time, t, and the point $x = P(t)$ is a measure of the position of the developing wave front in β. We expect that $\lim_{t\to\infty} (\mathrm{d}P/\mathrm{d}t) = v_n^*(D)$, the minimum travelling wave propagation speed. We now discuss the results of our numerical investigation of the initial-value problem (7), (8).

(*a*) $0 < D \ll 1$: *quadratic autocatalysis*, $n = 1$

The development of the concentrations α and β is illustrated in figure 1*a–e* for the typical case, $D = 0.01$, $\beta_0 = 0.1$, $\lambda = 10$, $p = 0$. We obtain similar solutions for $p = 1, 2, \ldots$. As t increases the solution has three distinct phases.

(i) *First induction phase*, $0 \leqslant t \leqslant t_1$

Figure 1*a* at $t = 2$ shows the initial development of the solution. In the centre of the initial-reaction region, $0 \leqslant x \leqslant \lambda$, the concentrations α and β decrease and increase, respectively, with reaction the dominant process. In the neighbourhood of the point $x = \lambda$, α increases with x to its initial value of unity. This higher value of α leads to a faster growth rate for β in the neighbourhood of $x = \lambda$, and a local maximum develops. There is also a small increase in β from its initial value of zero in the region $x > \lambda$ due to the slow diffusion of the autocatalyst, B. These processes continue as t increases and the concentration α tends to zero in the centre of the region $0 \leqslant x \leqslant \lambda$. The growth of β in the neighbourhood of the point $x = \lambda$ continues, driven by the diffusion of the reactant, A, into the region $0 \leqslant x \leqslant \lambda$, and a sharp spike-shaped maximum develops. This is shown in figure 1*b* at $t = 10$. During the

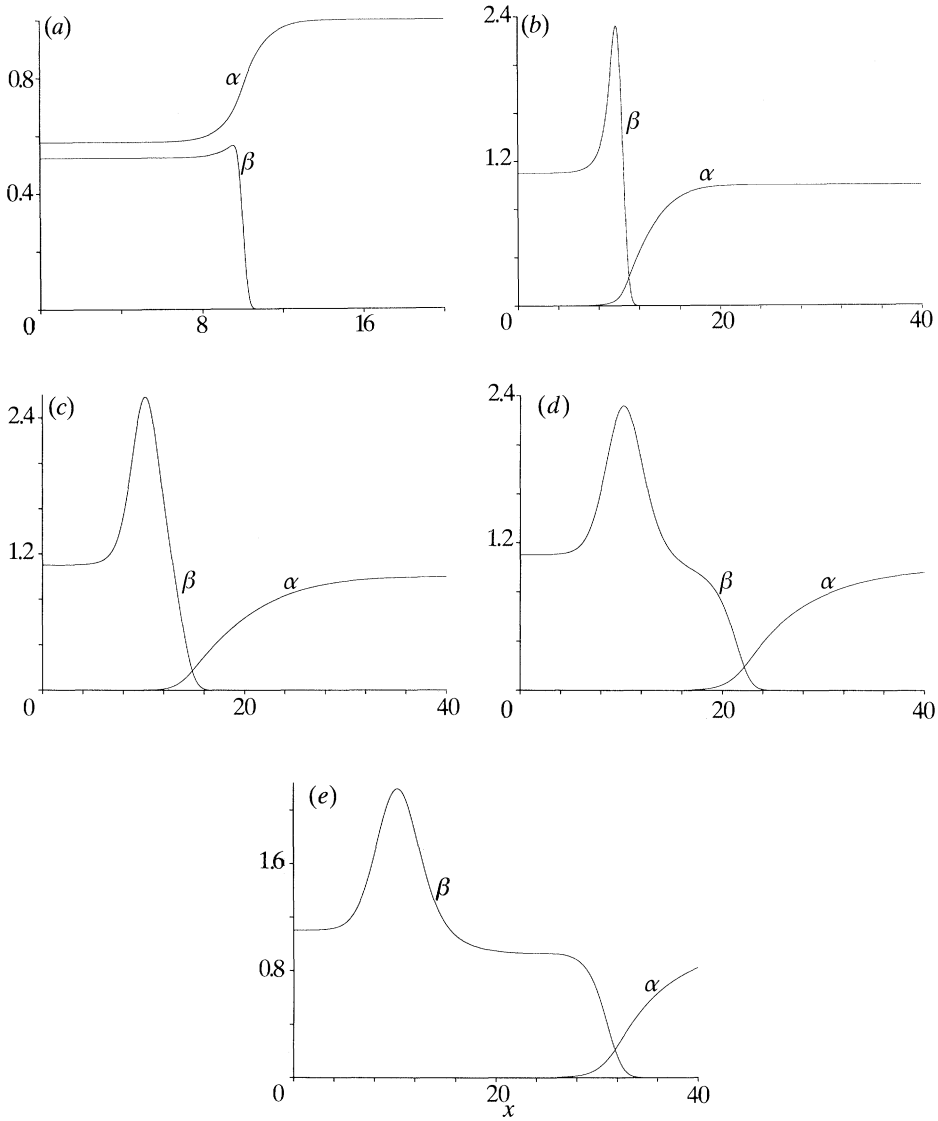

Figure 1. Graphs of the numerical solution of the initial-value problem (7), (8), with $n = 1$, $D = 0.01$, $\beta_0 = 0.1$, $\lambda = 10$, $p = 0$, when: (*a*) $t = 2$; (*b*) $t = 10$; (*c*) $t = 50$; (*d*) $t = 100$; (*e*) $t = 150$.

first induction phase, the autocatalyst, B, is effectively confined to the region $0 \leqslant x \leqslant \lambda$, and for $x > \lambda$, a significant concentration of B only exists in the immediate neighbourhood of $x = \lambda$, due to the slow diffusion. However, as t increases the diffusion of B starts to dominate the reaction in the spike and the rate of growth of the spike in β decreases. We consider that the first induction phase has ended when $\beta_{\max}(t)$, the greatest value of the concentration of B, reaches its maximum value, at $t = t_{\mathrm{I}}$. The duration of the first induction phase, t_{I}, is thus defined by

$$\mathrm{d}\beta_{\max}/\mathrm{d}t|_{t_{\mathrm{I}}} = 0. \tag{17}$$

The function $\beta_{\max}(t)$ is plotted in figure 2*a* for this case. We calculate t_{I} and $\beta_{\max}(t_{\mathrm{I}})$

PHILOSOPHICAL TRANSACTIONS OF THE ROYAL SOCIETY A MATHEMATICAL, PHYSICAL & ENGINEERING SCIENCES

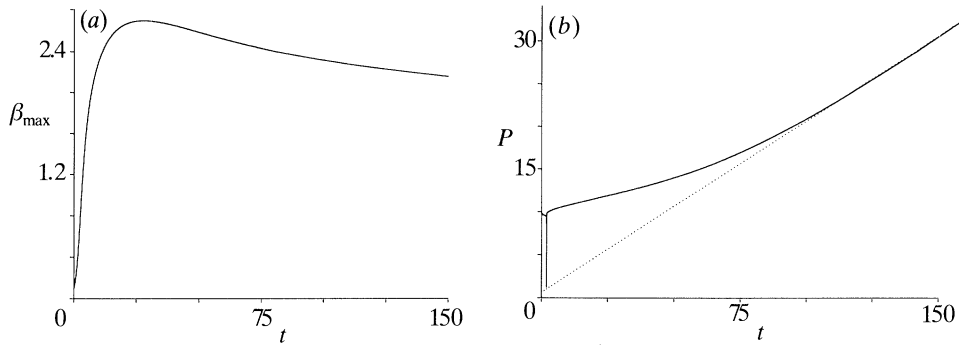

Figure 2. Graphs of the functions (*a*) $\beta_{max}(t)$ and (*b*) $P(t)$, calculated from the numerical solution of the initial-value problem (7), (8), with $n = 1$, $D = 0.01$, $\beta_0 = 0.1$, $\lambda = 10$, $p = 0$. The dotted line in (*b*) has slope $v_1^*(D)$.

Table 1. *The values of* t_I, $t_I\sqrt{D}$, β_{max} *and* $\beta_{max}\sqrt{D}$, *calculated from the numerical solution of the initial value problem* (7), (8), *with* $n = 1$, $\beta_0 = 0.1$, $\lambda = 10$ *and* $p = 0$ *for various values of* D

D	t_I	$t_I\sqrt{D}$	β_{max}	$\beta_{max}\sqrt{D}$
0.008	31.082	2.780	2.931	0.262
0.009	29.224	2.772	2.801	0.266
0.010	27.803	2.780	2.693	0.269
0.011	26.636	2.794	2.599	0.273

for various values of $D \ll 1$, with $\beta_0 = 0.1$, $\lambda = 10$ and $p = 0$. These are displayed in table 1, and indicate that $t_I = O(D^{-\frac{1}{2}})$ and $\beta_{max}(t_I) = O(D^{-\frac{1}{2}})$ as $D \to 0$, a result which we confirm in §4.

(ii) *Second induction phase,* $t_I \leqslant t \leqslant t_{II}$

During this phase the slow diffusion of the autocatalyst, B, into the region $x > \lambda$ becomes the dominant process in the spike in β. The width of the spike increases and $\beta_{max}(t)$ decreases with t. The concentration $\alpha \to 1$ as $x \to \infty$ over a length scale which increases as t increases. This process is illustrated in figure 1*c* at $t = 50$. The function $P(t)$ is monotone increasing for $t > t_I$ and asymptotes to a straight line with slope $v_1^*(D) = 2\sqrt{D}$, the minimum travelling wave propagation speed, as $t \to \infty$. Figure 2*b* is a graph of $P(t)$ for this case. As $t \to t_{II}$, the effect of the chemical reaction at the leading edge of the spike increases until a minimum speed travelling wave forms at $t = t_{II}$ when the effects of reaction and diffusion balance each other in the wave front. Figure 1*d* shows the travelling wave separating from the spike in β at $t = 100$. Although it is difficult to determine t_{II} accurately, our results indicate that $t_{II} = O(D^{-1})$ as $D \to 0$, a result which we confirm in §4.

(iii) *Travelling wave propagation,* $t \geqslant t_{II}$

The minimum speed permanent form travelling wave which forms at the end of the second induction phase propagates into the region $x > \lambda$ for $t \geqslant t_{II}$. Behind the wave front, the reactant, A, is completely consumed and diffusion alone acts on the concentration β. In particular, the spike in β slowly diffuses down to unity as $t \to \infty$. The solution at $t = 150$ is shown in figure 1*e*.

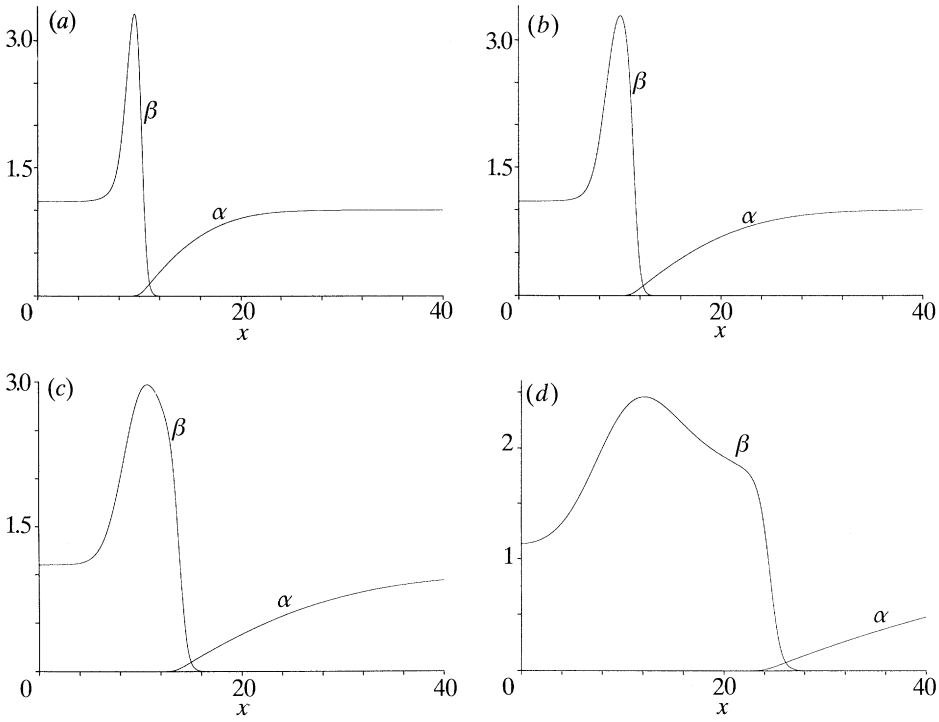

Figure 3. Graphs of the numerical solution of the initial-value problem (7), (8), with $n = 2$, $D = 0.01$, $\beta_0 = 0.1$, $\lambda = 10$, $p = 0$, when: (*a*) $t = 30$; (*b*) $t = 60$; (*c*) $t = 140$; (*d*) $t = 600$.

(*b*) $0 < D \ll 1$: *cubic autocatalysis*, $n = 2$
$p = 0$: $g(x)$ *is discontinuous at* $x = \lambda$

We consider the typical case, $D = 0.01$, $\beta_0 = 0.1$, $\lambda = 10$, and the development of the solution is illustrated in figure 3*a–d*. These show that there are four distinct phases in this case.

(i) *First induction phase*, $0 \leqslant t \leqslant t_{\mathrm{I}}$

The behaviour during this phase has the same qualitative features as outlined above for quadratic autocatalysis. In particular, a spike in β forms in the immediate neighbourhood of the point $x = \lambda$. This is shown in figure 3*a* at $t = 30$. A graph of the function $\beta_{\max}(t)$ is illustrated in figure 4*a*, and in table 2 the duration of the first induction phase, t_{I}, and the maximum concentration of the spike in β, $\beta_{\max}(t_{\mathrm{I}})$, are displayed for various values of $D \ll 1$, with $\beta_0 = 0.1$ and $\lambda = 10$. In §4 we demonstrate that $t_{\mathrm{I}} = O((\ln D)^2)$ and $\beta_{\max}(t_{\mathrm{I}}) = O(-D^{-\frac{1}{2}}(\ln D)^{-1})$, as $D \to 0$, consistent with these numerical results.

(ii) *Second induction phase*, $t_{\mathrm{I}} \leqslant t \leqslant t_{\mathrm{II}}$

During this phase the solution again shows the same qualitative features as described above for quadratic autocatalysis, with the spike in β spreading and $\beta_{\max}(t)$

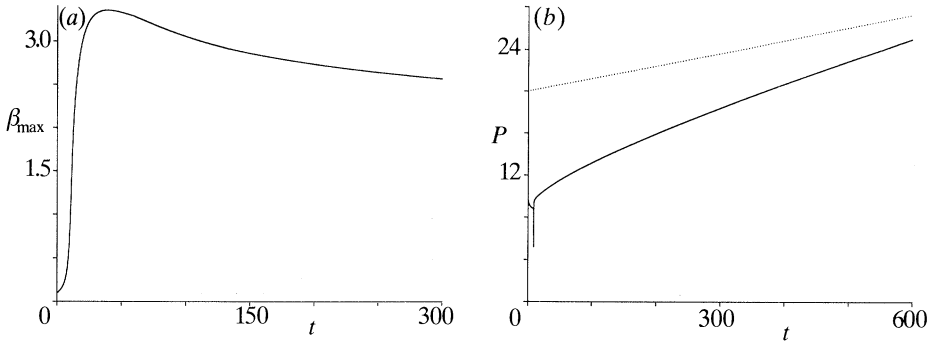

Figure 4. Graphs of the functions (*a*) $\beta_{max}(t)$ and (*b*) $P(t)$, calculated from the numerical solution of the initial-value problem (7), (8), with $n = 2$, $D = 0.01$, $\beta_0 = 0.1$, $\lambda = 10$, $p = 0$. The dotted line in (*b*) has slope $v_2^*(D)$.

Table 2. *The values of* t_I, $t_I(\ln D)^{-2}$, β_{max} *and* $\beta_{max} D^{\frac{1}{2}} \ln D$, *calculated from the numerical solution of the initial value problem* (7), (8), *with* $n = 2$, $\beta_0 = 0.1$, $\lambda = 10$ *and* $p = 0$ *for various values of* D

D	t_I	$t_I(\ln D)^{-2}$	β_{max}	$\beta_{max} D^{\frac{1}{2}} \ln D$
0.008	40.299	1.729	3.665	−1.583
0.009	39.659	1.787	3.500	−1.564
0.010	39.003	1.839	3.352	−1.544
0.011	38.755	1.905	3.228	−1.527

decreasing as t increases. This is illustrated in figure 3*b* at $t = 60$. However, in this case the wave front that emerges from the spike in β at $t = t_{II}$ does not separate from the spike, as shown by figure 3*c* at $t = 140$, shortly after t_{II}. For the illustrated solution, $t_{II} \approx 100$. The effect of the chemical reaction is negligible at the leading edge of the spike, and becomes significant only at the centre of the spike. Therefore, when the effects of reaction and diffusion balance they do so within the spike in β, which is where the wave-front forms.

(iii) *First travelling wave propagation phase,* $t_{II} \leqslant t \leqslant t_{III}$

The wave front that emerges at $t = t_{II}$ causes the spike in β to spread asymmetrically, propagating with speed $v > v_2^*(D)$, as shown by the graph of $P(t)$ in figure 4*b*. This wave front does not have the same structure as that found in a permanent form travelling wave solution, since the concentration β does not tend to unity as x decreases. However, as t increases, both the maximum value of β and the concentration gradient β_x in the wave front decrease slowly and the wave front decelerates to become a minimum-speed permanent-form travelling wave at $t = t_{III}$. We show in §4 that $t_{III} = O(D^{-2})$ and that $P(t_{III}) = O(D^{-1})$. This leads to $t_{III} = O(10^4)$ and $P(t_{III}) = O(100)$ for the illustrated solution. Although this is beyond the range of our numerical integration, the results obtained are not inconsistent with these order of magnitude estimates. The developing wave front is illustrated in figure 3*d* at $t = 600$. We also expect that during this phase the spike in β develops into a long hump, with width of $O(D^{-1})$ and maximum concentration of $O(1)$.

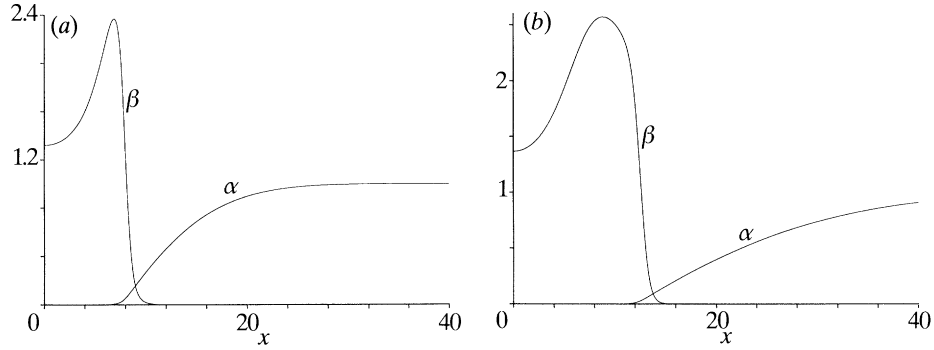

Figure 5. Graphs of the numerical solution of the initial-value problem (7), (8), with $n = 2$, $D = 0.01$, $\beta_0 = 0.1$, $\lambda = 10$, $p = 1$, when: (*a*) $t = 50$; (*b*) $t = 200$.

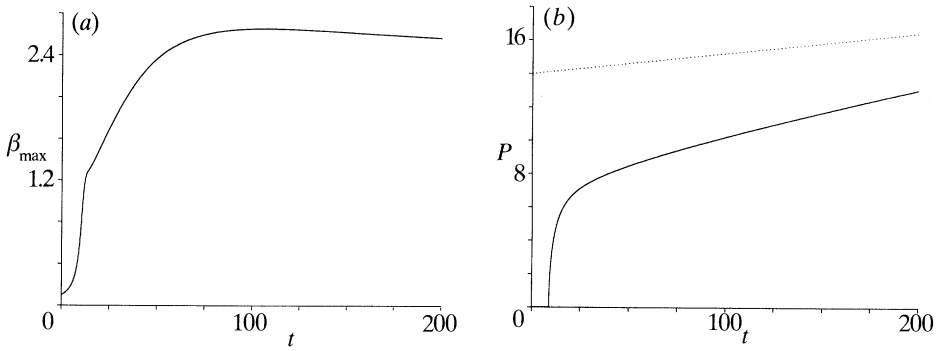

Figure 6. Graphs of the functions (*a*) $\beta_{\max}(t)$ and (*b*) $P(t)$, calculated from the numerical solution of the initial-value problem (7), (8), with $n = 2$, $D = 0.01$, $\beta_0 = 0.1$, $\lambda = 10$, $p = 1$. The dotted line in (*b*) has slope $v_2^*(D)$.

(iv) *Second travelling wave propagation phase, $t \geqslant t_{\mathrm{III}}$*

We expect that the minimum speed travelling wave propagates away to infinity during this phase and that the hump in β slowly diffuses down to unity.

$p = 1, 2, \ldots$: $g(x)$ is continuous at $x = \lambda$

The solution for $p = 1, 2, \ldots$ differs from that described above for $p = 0$ in two respects. First, the spike in β does not develop in the immediate neighbourhood of the point $x = \lambda$, where β is small and the rate of reaction is not sufficient to generate the spike. In addition, the second induction phase is absent with $t_{\mathrm{I}} = t_{\mathrm{II}}$. The solution in the typical case, $D = 0.01$, $\beta_0 = 0.1$, $\lambda = 10$, $p = 1$ is illustrated in figure 5*a*, *b* at $t = 50$ and 200 respectively. The development of the solution for $t \geqslant t_{\mathrm{II}}$ is as outlined above in the case $p = 0$. Graphs of the functions $\beta_{\max}(t)$ and $P(t)$ are shown in figure 6 *a*, *b* respectively.

We now turn our attention to numerical solutions of the initial value problem (7), (8) with $D = 0$.

(*c*) *$D = 0$: quadratic autocatalysis, $n = 1$*

The numerical results, outlined above for the case $0 < D \ll 1$, indicate that the duration of the first induction phase, $t_{\mathrm{I}} \to \infty$ as $D \to 0$, and hence that when $D = 0$ this

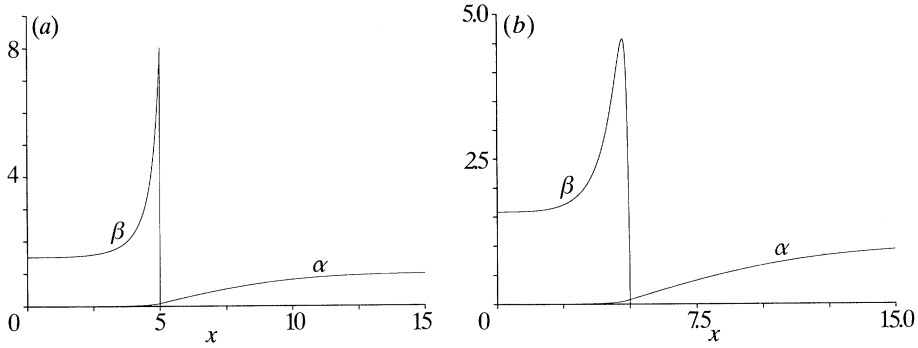

Figure 7. Graphs of the numerical solution of the initial-value problem (7), (8), with $n = 1$, $D = 0$, $\beta_0 = 0.5$, $\lambda = 5$ and (*a*) $p = 0$, $t = 10$, (*b*) $p = 1$, $t = 20$.

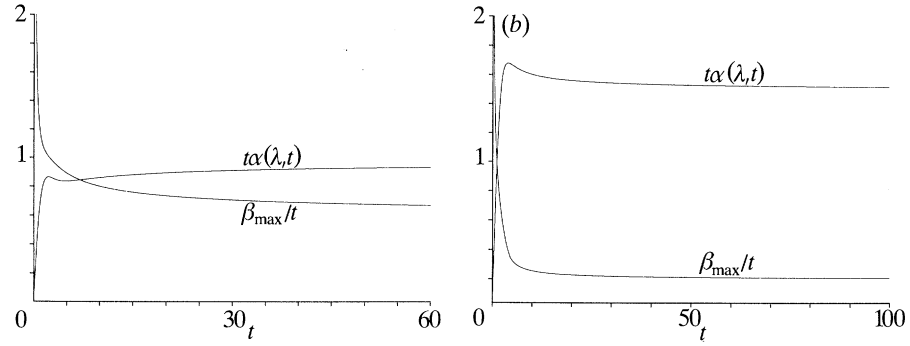

Figure 8. Graphs of the functions $t\alpha(\lambda, t)$ and $t^{-1}\beta_{\max}(t)$, calculated from the numerical solution of the initial-value problem (7), (8), with $n = 1$, $D = 0$, $\beta_0 = 0.5$, $\lambda = 5$ and (*a*) $p = 0$, (*b*) $p = 1$.

phase is indefinitely long and no travelling wave forms. The numerical solutions, which we obtain when $D = 0$ confirm this prediction. The solutions in the two typical cases, $\beta_0 = 0.5$, $\lambda = 5$, $p = 0, 1$ are illustrated in figure 7*a*, *b* at $t = 10$ and $t = 20$ respectively. These show that a sharp spike in β develops at the point $x = \lambda$ for $p = 0$, and in the immediate neighbourhood of $x = \lambda$ for $p = 1$. The autocatalyst, B, is confined to the region $0 \leqslant x \leqslant \lambda$, and the spike in β grows indefinitely. These solutions suggest that $\beta_{\max} = O(t)$ and $\alpha(\lambda, t) = O(t^{-1})$, which we confirm analytically in §3. The functions $t\alpha(\lambda, t)$ and $t^{-1}\beta_{\max}(t)$ asymptote to constant values as $t \to \infty$ and are plotted in figure 8*a*, *b* for $p = 0$ and $p = 1$ respectively. We obtain similar solutions for $p = 2, 3, \ldots$.

(*d*) $D = 0$: *cubic autocatalysis*, $n = 2$

$p = 0$: $g(x)$ *is discontinuous at* $x = \lambda$

The solution when $t = 5$ in the typical case, $\beta_0 = 0.5$, $\lambda = 5$ is illustrated in figure 9. This shows that a sharp spike in β develops at $x = \lambda$ and grows much more rapidly than in the case of quadratic autocatalysis. This growth is so rapid and the spike becomes so narrow that, with the computer time available to us, it is not possible to obtain accurate results for $t \geqslant 5$ in this case. In §3 we demonstrate analytically that $\alpha(\lambda, t) = O(t^{-\frac{1}{2}} e^{-2\sigma t^{\frac{1}{2}}})$, $\beta_{\max}(t) = O(e^{2\sigma t^{\frac{1}{2}}})$ and the width of the spike is of $O(e^{-2\sigma t^{\frac{1}{2}}})$ as

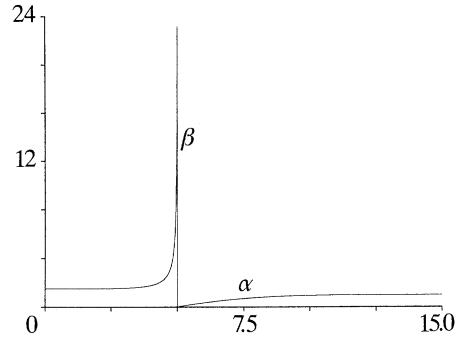

Figure 9. A graph of the numerical solution of the initial-value problem (7), (8), with $n = 2$, $D = 0$, $\beta_0 = 0.5$, $\lambda = 5$, $p = 0$, when $t = 5$.

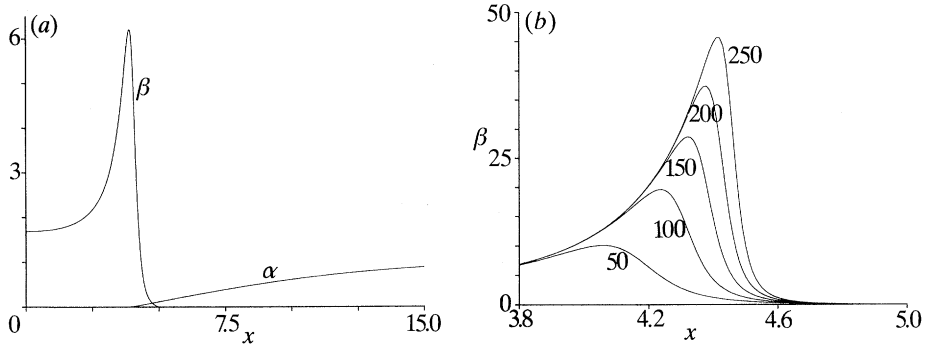

Figure 10. Graphs of the numerical solution of the initial value problem (7), (8), with $n = 2$, $D = 0$, $\beta_0 = 0.5$, $\lambda = 5$, $p = 1$, when (*a*) $t = 30$, (*b*) $t = 50$, 100, 150, 200, 250.

$t \to \infty$, where σ is a positive constant. The numerical results that we present are consistent with exponential decay and growth of the concentrations α and β, respectively, but not accurate enough to determine σ.

$p = 1, 2, \ldots$: $g(x)$ *is continuous at* $x = \lambda$

The solution in the typical case $\beta_0 = 0.5$, $\lambda = 5$, $p = 1$ is illustrated in figure 10*a* at $t = 30$. This shows that a spike in β again forms, but not in the immediate neighbourhood of the point $x = \lambda$. Near this point, the concentration β is small and therefore the rate of reaction, which is of $O(\alpha\beta^2)$, is not sufficient to generate a spike. The behaviour of the concentration β is illustrated in figure 10*b* at $t = 50$, 100, 150, 200, 250, which clearly shows that the leading edge of the spike in β steepens and moves towards $x = \lambda$ as t increases. We wish to determine the position of the spike as t increases and to this end define the function $x_{\max}(t)$ by $\beta(x_{\max}, t) = \beta_{\max}(t)$. The functions $\beta_{\max}(t)$ and $x_{\max}(t)$ are plotted in figure 11*a*, *b* respectively. We find that $\beta_{\max}(t) = O(t^m)$ as $t \to \infty$, where $m \equiv m(p)$ is given in table 3 for $1 \leqslant p \leqslant 5$, and $x_{\max}(t)$ increases very slowly as t increases. We discuss the behaviour of $x_{\max}(t)$ as $t \to \infty$ in §3. For $p = 2, 3, \ldots$, the solution behaves in the same manner, although the spike in β forms further from the point $x = \lambda$ as p increases.

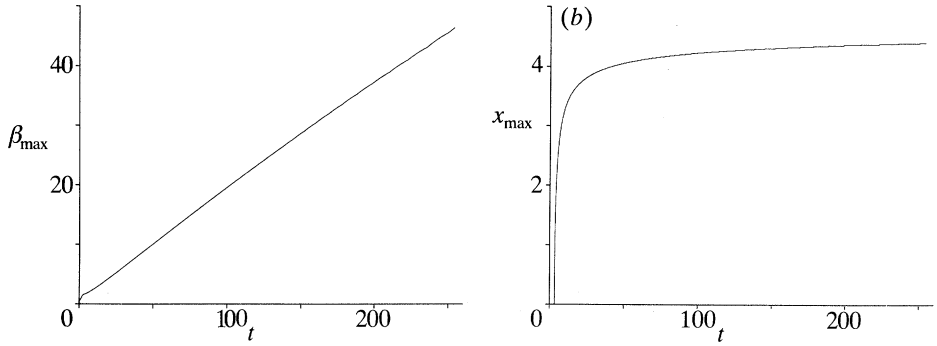

Figure 11. Graphs of the functions (*a*) $\beta_{max}(t)$ and (*b*) $x_{max}(t)$, calculated from the numerical solution of the initial-value problem (7), (8), with $n = 2$, $D = 0$, $\beta_0 = 0.5$, $\lambda = 5$, $p = 1$.

Table 3. *The value of the constant m, calculated from the numerical solution of the initial value problem (7), (8), with* $D = 0$, $n = 2$, $\beta_0 = 0.5$, $\lambda = 5$ *for* $1 \leqslant p \leqslant 5$

p	$m(p)$
1	0.96
2	0.83
3	0.80
4	0.77
5	0.73

In the following section, we obtain an asymptotic solution of (11), (12), (13), the initial-value problem with $D = 0$, for $t \gg 1$. The asymptotic solution for $t \ll 1$ can be found in Billingham (1990).

3. Asymptotic solution of the initial-value problem with $D = 0$ for $t \gg 1$

The numerical solutions of the initial-value problem (11), (12), (13), which we described in §2, reveal that for $t \gg 1$ there are two distinct regions in $0 < x \leqslant \lambda$, where the behaviour of the solution is entirely different. This is shown clearly in figures 7*a*, *b* and 9 for three typical cases where it can be seen that $\beta \gg 1$, $\alpha_- \ll 1$ for $0 \leqslant (\lambda - x) \ll 1$, and $\beta = O(1)$, $\alpha_- = o(1)$ for $0 < (\lambda - x) = O(1)$ as $t \to \infty$. In this section, we construct asymptotic solutions of the initial-value problem, based on this structure, for t large. However, we find that such an asymptotic solution does not exist under cubic autocatalysis if $g(x)$ is continuous at $x = \lambda$. This result is supported by the numerical solution when $p = 1, 2, \ldots$, a typical example of which is shown in figure 10*a*. In this case, the spike in β forms away from the immediate neighbourhood of $x = \lambda$ and drifts very slowly towards the point $x = \lambda$.

To proceed we first consider the solution of the initial-value problem (11) for $t \geqslant 0$, with the boundary condition at $x = \lambda$ given by $\alpha_+(\lambda, t) = A(t)$, which is to be determined. The initial condition (11*b*) fixes $A(0) = 1$, whilst the above discussion implies that

$$A(t) \to 0, \quad \text{as} \quad t \to \infty. \tag{18}$$

The solution of equation (11*a*) subject to the above condition at $x = 0$ and conditions (11*b*, *c*) is readily obtained, via Laplace transforms, as

$$\alpha_+(x,t) = \operatorname{erf}\left(\frac{x-\lambda}{2t^{\frac{1}{2}}}\right) + \frac{2}{\sqrt{\pi}} \int_{\frac{(x-\lambda)}{2t^{\frac{1}{2}}}}^{\infty} A\left\{t - \frac{(x-\lambda)^2}{4\omega^2}\right\} \mathrm{e}^{-\omega^2}\, \mathrm{d}\omega, \quad \text{for} \quad x \geqslant \lambda, \quad t \geqslant 0. \tag{19}$$

An asymptotic analysis of equation (19) for $t \gg 1$ (the details of which are given in Billingham (1991)) shows that

$$(\partial \alpha_+ / \partial x)(\lambda, t) = (1/(\pi t)^{\frac{1}{2}}) + o(1/t^{\frac{1}{2}}), \quad \text{as} \quad t \to \infty. \tag{20}$$

We now turn our attention to the solution of equations (12*a*, *b*) in the reaction domain, $0 \leqslant x \leqslant \lambda$. The numerical solutions, discussed above, indicate that this develops in two asymptotic regions as $t \to \infty$. We label the thin region close to $x = \lambda$ as region I(*a*), and the region exterior to this as region I(*b*). We then have that

$$\text{in region I}(a), \qquad 0 < (\lambda - x) = o(1), \quad \alpha_- = o(1), \quad \beta^{-1} = o(1), \tag{21}$$

$$\text{in region I}(b), \; 0 < (\lambda - x) = O(1), \quad \alpha_- = o(1), \quad \beta = O(1) \quad \text{as} \quad t \to \infty. \tag{22}$$

We consider first the development in region I(*a*). Appropriate scaled variables in region I(*a*) are

$$\left.\begin{aligned} \alpha_-(x,t) &= \phi_n(t)\, F^{(n)}(\bar{x}^{(n)}, t), \\ \beta(x,t) &= \psi_n(t)\, G^{(n)}(\bar{x}^{(n)}, t), \\ x &= \lambda - \chi_n(t)\, \bar{x}^{(n)}, \end{aligned}\right\} \tag{23}$$

where

$$\left.\begin{aligned} \phi_n(t) = o(1), \quad \psi_n^{-1}(t) = o(1), \quad \chi_n(t) = o(1), \\ F^{(n)}(\bar{x}^{(n)}, t) = O(1), \quad G^{(n)}(\bar{x}^{(n)}, t) = O(1), \quad \bar{x}^{(n)} = O(1) \quad \text{as} \quad t \to \infty, \end{aligned}\right\} \tag{24}$$

with $n = 1, 2$, for quadratic and cubic autocatalysis respectively. On using expression (20) and the connection condition (13*b*), we obtain $\chi_n(t) = O(t^{\frac{1}{2}}\phi_n(t))$ as $t \to \infty$ and, without loss of generality, we define

$$\chi_n(t) = t^{\frac{1}{2}}\phi_n(t). \tag{25}$$

We now substitute for α_-, β and x from (23) into equations (12*a*, *b*), which become, after using (25)

$$F_t^{(n)} - \left(\frac{1}{2t} + \frac{\phi_{nt}}{\phi_n}\right) \bar{x}^{(n)} F_{\bar{x}}^{(n)} + \frac{\phi_{nt}}{\phi_n} F^{(n)} = \frac{1}{t\phi_n^2} F_{\bar{x}\bar{x}}^{(n)} - \psi_n^n F^{(n)} G^{(n)^n}, \tag{26}$$

$$G_t^{(n)} - \left(\frac{1}{2t} + \frac{\phi_{nt}}{\phi_n}\right) \bar{x}^{(n)} G_{\bar{x}}^{(n)} + \frac{\psi_{nt}}{\psi_n} G^{(n)} = \phi_n \psi_n^{n-1} F^{(n)} G^{(n)^n}. \tag{27}$$

With $\phi_n(t) = o(1)$ as $t \to \infty$, it is readily shown that $\phi_{nt}/\phi_n = o(1/t\phi_n^2)$ as $t \to \infty$. The leading order balance in equation (26) is thus between the reaction and diffusion terms on the right hand side. This requires that $\phi_n(t) = O(1/t^{\frac{1}{2}}\psi_n^{\frac{1}{2}n}(t))$, as $t \to \infty$. Without loss of generality, we take

$$\phi_n(t) = t^{-\frac{1}{2}}\psi_n^{-\frac{1}{2}n}(t). \tag{28}$$

On using (28), a leading order balance of terms in equation (27) is obtained when $\psi_{n_t}(t) = O(t^{-\frac{1}{2}}\psi_n^{\frac{1}{2}n}(t))$, as $t \to \infty$. Thus we have that

$$\psi_{n_t} = \sigma t^{-\frac{1}{2}}\psi_n^{\frac{1}{2}n}, \tag{29}$$

for some positive constant σ. With $n = 1$, an integration of (29) leads to $\psi_1(t) = O(t)$ as $t \to \infty$, and we take $\psi_1(t) = t$. For $n = 2$, however, an integration of (29) gives $\psi_2(t) = O(\mathrm{e}^{2\sigma t^{\frac{1}{2}}})$ and we put $\psi_2(t) = \mathrm{e}^{2\sigma t^{\frac{1}{2}}}$. The scalings in region I(a) are, therefore

$$\chi_1(t) = t^{-\frac{1}{2}}, \quad \phi_1(t) = t^{-1}, \quad \psi_1(t) = t, \quad n = 1, \tag{30a}$$

$$\chi_2(t) = \mathrm{e}^{-2\sigma t^{\frac{1}{2}}}, \quad \phi_2(t) = t^{-\frac{1}{2}}\,\mathrm{e}^{-2\sigma t^{\frac{1}{2}}}, \quad \psi_2(t) = \mathrm{e}^{2\sigma t^{\frac{1}{2}}}, \quad n = 2. \tag{30b}$$

These scalings show that the spike in β, which develops as $t \to \infty$, is exponentially thin and has an exponentially large maximum concentration under cubic autocatalysis, whereas these quantities are only algebraically small and large, respectively, in the case of quadratic autocatalysis. These differences are apparent in the numerical solutions illustrated in figures 7a, b and 9. We now consider separately the two cases of quadratic and cubic autocatalysis.

(a) *Quadratic autocatalysis*, $n = 1$

Under quadratic autocatalysis, equations (26), (27) are

$$t^{-2}(tF_t + \tfrac{1}{2}\bar{x}F_{\bar{x}} - F) = F_{\bar{x}\bar{x}} - FG, \tag{31a}$$

$$tG_t + \tfrac{1}{2}\bar{x}G_{\bar{x}} + G = FG, \tag{31b}$$

where

$$\alpha_-(x,t) = t^{-1}F^{(1)}(\bar{x}^{(1)},t), \quad \beta(x,t) = tG^{(1)}(\bar{x}^{(1)},t), \quad x = \lambda - t^{-\frac{1}{2}}\bar{x}^{(1)}. \tag{32}$$

In equations (31a, b), we have omitted the bracketed superscripts for convenience of notation. At leading order, equations (31) become

$$F_{0_{\bar{x}\bar{x}}} = F_0 G_0, \quad \tfrac{1}{2}\bar{x}G_{0_{\bar{x}}} + G_0 = F_0 G_0, \tag{33a, b}$$

where $F(\bar{x},t) = F_0(\bar{x}) + o(1)$, $G(\bar{x},t) = G_0(\bar{x}) + o(1)$ as $t \to \infty$. In order to match with the solution in region I(b), where $\alpha_- = o(1)$ and $\beta = O(1)$, we require that

$$F_0(\bar{x}) = o(\bar{x}^2), \quad G_0(\bar{x}) = O(\bar{x}^{-2}) \quad \text{as} \quad \bar{x} \to \infty. \tag{34a, b}$$

The connection conditions (13a, b) must also be satisfied at $\bar{x} = 0$. On using (32), we find that

$$A(t) \sim A_\infty^{(1)}\, t^{-1} \quad \text{as} \quad t \to \infty, \tag{35}$$

for some positive constant $A_\infty^{(1)}$. Condition (13a) then requires that

$$F_0(0) = A_\infty, \tag{36a}$$

omitting the superscript for convenience of notation, and condition (13b) reduces, via (20) and (32) to

$$F_{0_{\bar{x}}}(0) = -1/\sqrt{\pi}. \tag{36b}$$

In addition, equation (10a) shows that, as $x \to \lambda^-$, $\beta(x,t)$ has the same degree of smoothness as the initial input function, $g(x)$, for all $t \geqslant 0$. In particular, from equation (8d), $\beta(x,t) = O((\lambda - x)\,p)$ as $x \to \lambda^-$, and hence

$$G_0(\bar{x}) = O(\bar{x}p) \quad \text{as} \quad \bar{x} \to 0. \tag{37}$$

After subtracting equation (33a) from (33b) the resulting equation can be integrated once to give

$$\bar{x}F_{0_{\bar{x}}} = F_0 + \tfrac{1}{2}\bar{x}^2 G_0 - A_\infty, \tag{38}$$

via condition (36a). On defining new variables as

$$\hat{F}_0 = F_0, \quad \hat{G}_0 = \bar{x}^2 G_0, \quad \bar{x} = \mathrm{e}^s, \tag{39}$$

equations (33b) and (38) are reduced to the second-order autonomous system

$$\hat{F}_{0s} = \hat{F}_0 + \tfrac{1}{2}\hat{G}_0 - A_\infty, \quad \hat{G}_{0s} = 2\hat{F}_0\,\hat{G}_0. \tag{40a, b}$$

We require a solution of equations (40), subject to the boundary conditions (34), (36), (37), which become

$$\hat{F}_0(s) = o(\mathrm{e}^{2s}), \quad \hat{G}_0(s) = O(1) \quad \text{as} \quad s \to \infty, \tag{41a, b}$$

$$\hat{F}_0(s) \to A_\infty, \quad \hat{F}_{0s}(s) \sim -\mathrm{e}^s/\sqrt{\pi}, \quad \hat{G}_0(s) = O(\mathrm{e}^{(p+2)s}) \quad \text{as} \quad s \to -\infty. \tag{42a–c}$$

The system of equations (40) has just two finite equilibrium points at $(0, 2A_\infty)$ and $(A_\infty, 0)$ in the $(\hat{F}_0, \hat{G}_0)$ phase plane. The point $(0, 2A_\infty)$ is a saddle with eigenvalues and associated eigenvectors

$$\mu_1 = \tfrac{1}{2}\{1 - \sqrt{(1 + 8A_\infty)}\}, \quad \boldsymbol{e}_{\mu_1} = (\mu_1, 4A_\infty)^{\mathrm{T}}, \tag{43a}$$

$$\mu_2 = \tfrac{1}{2}\{1 + \sqrt{(1 + 8A_\infty)}\}, \quad \boldsymbol{e}_{\mu_2} = (\mu_2, 4A_\infty)^{\mathrm{T}}. \tag{43b}$$

The point $(A_\infty, 0)$ is an unstable node with eigenvalues and associated eigenvectors

$$\nu_1 = 1, \quad \boldsymbol{e}_{\nu_1} = (1, 0)^{\mathrm{T}}, \tag{44a}$$

$$\nu_2 = 2A_\infty, \quad \boldsymbol{e}_{\nu_2} = (1, 4A_\infty - 2)^{\mathrm{T}}. \tag{44b}$$

We now show that there exists a unique integral path which connects the two equilibrium points in the first quadrant of the $(\hat{F}_0, \hat{G}_0)$ phase plane. We define the closed region R by

$$R = \{(\hat{F}_0, \hat{G}_0) \colon 0 \leqslant \hat{F}_0 \leqslant A_\infty - \tfrac{1}{2}\hat{G}_0, \quad 0 \leqslant \hat{G}_0 \leqslant 2A_\infty\}. \tag{45}$$

From (43a), the stable separatrix of the point $(0, 2A_\infty)$ with $\hat{F}_0 \geqslant 0$, which we label as S_1, lies in the region R in the neighbourhood of $(0, 2A_\infty)$. However, equations (40) show that no integral path is directed strictly into the region R on its boundary. The stable separatrix, S_1, therefore originates in the region R, and the only possibility is that it leaves the point $(A_\infty, 0)$. The phase portrait of the system of equations (40) is sketched in figure 12. An integral path which satisfies conditions (41b) and (42a) must originate at the point $(A_\infty, 0)$ and have $\hat{G}_0$ bounded as $s \to \infty$. The only such path is S_1, which connects the two equilibrium points. After applying condition (42b) the solution is uniquely determined in terms of the constants A_∞ and p, and has the asymptotic properties

$$\hat{F}_0(s) \sim -\mu_1 C(A_\infty, p)\,\mathrm{e}^{\mu_1 s}, \tag{46a}$$

$$\hat{G}_0(s) \sim 2A_\infty - 4A_\infty C(A_\infty, p)\,\mathrm{e}^{\mu_1 s}, \quad \text{as} \quad s \to \infty, \tag{46b}$$

$$\hat{F}_0(s) \sim A_\infty - e^s/\sqrt{\pi} + B(A_\infty, p)\,\mathrm{e}^{2A_\infty s}, \tag{47a}$$

$$\hat{G}_0(s) \sim (4A_\infty - 2)\,B(A_\infty, p)\,\mathrm{e}^{2A_\infty s}, \quad \text{as} \quad s \to -\infty, \tag{47b}$$

where C and B are fixed in terms of A_∞ and p. Condition (41a) is satisfied by $\hat{F}_0(s)$, but in order to satisfy condition (42c) we further require that

$$A_\infty = \tfrac{1}{2}(p + 2), \tag{48}$$

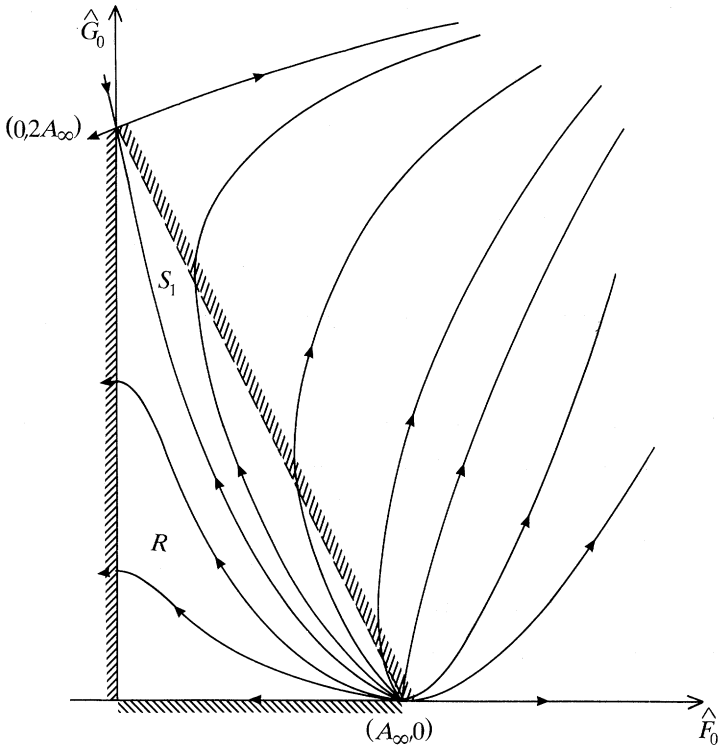

Figure 12. A sketch of the phase portrait of the system of equations (40).

Table 4. *The values of the constants B and C, calculated from the numerical solution of equations (75) for p = 0, 1, 2, 3*

p	$B(p)$	$C(p)$
0	0.32	1.77
1	0.15	2.70
2	0.05	4.74
3	0.02	8.65

after which all conditions have been satisfied. We calculate the equation of S_1 numerically for $p = 0, 1, 2, 3$ by integrating the equations (40) with a fourth order Runge–Kutta method. This enables us to determine $B(p)$ and $C(p)$, which are displayed in table 4.

We have now shown that

$$\alpha_- \sim -t^{-1}\mu_1 C(p)\,\bar{x}^{\mu_1}, \tag{49a}$$

$$\beta \sim t\{(p+2)\,\bar{x}^{-2} - 2(p+2)\,C(p)\,\bar{x}^{-2+\mu_1}\}, \quad \text{with} \quad \bar{x} \gg 1 \quad \text{as} \quad t \to \infty, \tag{49b}$$

$$\alpha_- \sim t^{-1}\{\tfrac{1}{2}(p+2) - \bar{x}/\sqrt{\pi} + B(p)\,\bar{x}^{p+2}\}, \tag{50a}$$

$$\beta \sim 2t(p+1)\,B(p)\,\bar{x}^{p}, \quad \text{with} \quad \bar{x} \ll 1 \quad \text{as} \quad t \to \infty, \tag{50b}$$

where $\mu_1 = \frac{1}{2}\{1 - \sqrt{(4p+9)}\}$, from (43*a*) and (48). The approximations (50) clearly

remain uniform as $\bar{x} \to 0$. The approximation (49b), however, becomes non-uniform when $\bar{x} = O(t^{\frac{1}{2}})$, or $\lambda - x = O(1)$, and we approach region I(b). Approximations (49) demonstrate that $\alpha_-(x,t) = O(t^{\frac{1}{2}\mu_1 - 1})$ and $\beta(x,t) = O(1) + O(t^{\frac{1}{2}\mu_1})$. Appropriate scaled variables in region I(b) are, therefore

$$\alpha_-(x,t) = t^{\frac{1}{2}\mu_1 - 1}\,\gamma^{(1)}(x,t), \quad \beta(x,t) = \beta_\infty^{(1)}(x) + t^{\frac{1}{2}\mu_1}\theta^{(1)}(x,t). \tag{51a, b}$$

In terms of the scaled variables (51), equations (12a, b) become, at leading order as $t \to \infty$

$$\gamma_{0xx} = \beta_\infty\,\gamma_0, \quad \mu_1\,\theta_0 = \beta_\infty\,\gamma_0, \tag{52a, b}$$

where $\gamma^{(1)}(x,t) = \gamma_0(x) + o(1)$ and $\theta^{(1)}(x,t) = \theta_0(x) + o(1)$, as $t \to \infty$. Matching with region I(a) leads to the boundary conditions

$$\left.\begin{aligned} \gamma_0(x) &\sim \mu_1\,C(p)\,(\lambda - x)^{\mu_1} && (53a)\\ \theta_0(x) &\sim 2(p+2)\,C(p)\,(\lambda - x)^{-2+\mu_1}, && (53b)\\ \beta_\infty(x) &\sim (p+2)\,(\lambda - x)^{-2}, && (53c) \end{aligned}\right\} \quad \text{as} \quad x \to \lambda^-.$$

Condition (12d) also requires that

$$(\mathrm{d}\gamma_0/\mathrm{d}x)\,(0) = (\mathrm{d}\theta_0/\mathrm{d}x)\,(0) = 0. \tag{54}$$

The function $\beta_\infty(x)$ cannot be determined by the asymptotic analysis as $t \to \infty$ and depends upon the initial conditions (12c). However, equations (52) and boundary conditions (53a, b) and (54) determine $\gamma_0(x)$ and $\theta_0(x)$ uniquely for any strictly positive function $\beta_\infty(x)$ which satisfies conditions (53c) and $\beta_\infty'(0) = 0$. This completes the asymptotic analysis for $t \gg 1$ under quadratic autocatalysis.

To summarize, in region I(a), $0 \leqslant (\lambda - x) = O(t^{-\frac{1}{2}})$, and

$$\alpha_- = t^{-1}F_0(\bar{x}) + o(t^{-1}), \quad \beta = tG_0(\bar{x}) + o(t), \tag{55a, b}$$

where the functions $F_0(\bar{x})$ and $G_0(\bar{x})$ are the unique solution of the boundary value problem (33), (34), (36), (37). As illustrations, we calculate the functions $F_0(\bar{x})$ and $G_0(\bar{x})$ numerically for the cases $p = 0$ and $p = 1$. We integrate equations (40) using a fourth order Runge–Kutta method and $t^{-1}F_0(\bar{x}), tG_0(\bar{x})$ are plotted in figure 13a, b for $p = 0$, $t = 10$ and $p = 1$, $t = 20$ respectively. By comparison, figure 7a, b shows the corresponding solutions of the full initial-value problem (11), (12), (13). These have the same functional form in region I(a) as that exhibited by $t^{-1}F_0$ and tG_0 and also display the predicted algebraic decay and growth of α_- and β respectively, and algebraic thinning of the width of the spike in β. Figure 8a, b shows $t\alpha(\lambda, t)$ and $t^{-1}\beta_{\max}(t)$ for $p = 0$ and $p = 1$, which asymptote to the constant values, $\frac{1}{2}(p+2)$ and $\sup_{0 \leqslant \bar{x} < \infty} G_0(\bar{x})$, respectively, as $t \to \infty$. This is in agreement with the predictions of the present asymptotic theory.

In region I(b), $0 < (\lambda - x) = O(1)$, and

$$\alpha_- = t^{\frac{1}{2}\mu_1 - 1}\,\gamma_0(x) + o(t^{\frac{1}{2}\mu_1 - 1}), \quad \beta = \beta_\infty(x) + t^{\frac{1}{2}\mu_1}\,\theta_0(x) + o(t^{\frac{1}{2}\mu_1}), \tag{56a, b}$$

where the functions $\gamma_0(x)$ and $\theta_0(x)$ are the unique solutions of the boundary-value problem (52), (53), (54). The solution thus depends upon the initial conditions (12c) in region I(b), with β steady up to $O(t^{\frac{1}{2}\mu_1})$, $\beta \sim (p+2)(\lambda - x)^{-2}$ as $x \to \lambda^-$, and $\alpha_- = O(t^{\frac{1}{2}\mu_1 - 1})$ as $t \to \infty$. This structure is clearly displayed in figure 7a, b. Finally, we have, via (35), (48), that

$$A(t) \sim \tfrac{1}{2}(p+2)\,t^{-1} \quad \text{as} \quad t \to \infty, \tag{56c}$$

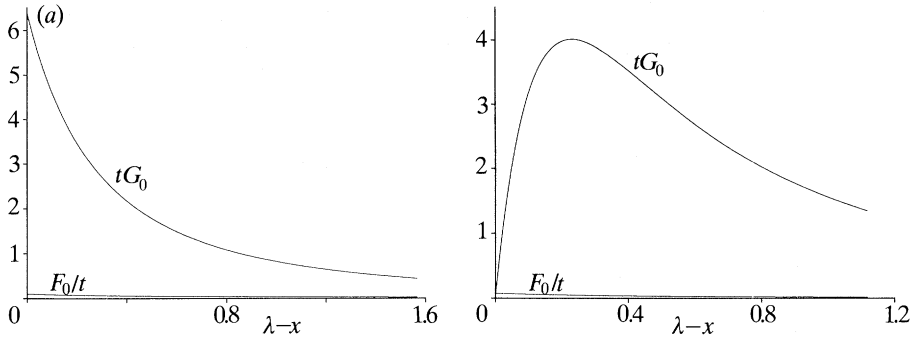

Figure 13. Graphs of the functions $t^{-1}F_0(x)$ and $tG_0(x)$, calculated from the numerical solution of equations (40), when (*a*) $p = 0$, $t = 10$, (*b*) $p = 1$, $t = 20$.

and we can then readily obtain the long-time behaviour of $\alpha_+(x,t)$ in $x > \lambda$ as

$$\alpha_+ \sim \operatorname{erf}(\tfrac{1}{2}\eta) + t^{-1}\tfrac{1}{2}(p+2)\left(1 - \tfrac{1}{2}\eta\, \mathrm{e}^{-\frac{1}{4}\eta^2}\int_0^\eta \mathrm{e}^{\frac{1}{4}s^2}\,\mathrm{d}s + k\eta\, \mathrm{e}^{-\frac{1}{4}\eta^2}\right), \tag{56d}$$

where $\eta = (x-\lambda)t^{-\frac{1}{2}}$ and k is a constant which is determined by higher order terms in the expansion of $F(\bar{x},t)$.

(*b*) *Cubic autocatalysis*, $n = 2$

We consider first the development of the solution in region I(*a*), $0 < (\lambda - x) = O(\mathrm{e}^{-2\sigma t^{\frac{1}{2}}})$. Under cubic autocatalysis equations (26), (27) become

$$t^{-\frac{1}{2}}\,\mathrm{e}^{-4\sigma t^{\frac{1}{2}}}\{t^{\frac{1}{2}}F_t + \sigma\bar{x}F_{\bar{x}} - F) - \tfrac{1}{2}t^{-\frac{1}{2}}F\} = F_{\bar{x}\bar{x}} - FG^2, \tag{57a}$$

$$t^{\frac{1}{2}}G_t + \sigma(\bar{x}G_{\bar{x}} + G) = FG^2, \tag{57b}$$

where

$$\alpha_-(x,t) = t^{-\frac{1}{2}}\,\mathrm{e}^{-2\sigma t^{\frac{1}{2}}}F^{(2)}(\bar{x}^{(2)},t), \quad \beta(x,t) = \mathrm{e}^{2\sigma t^{\frac{1}{2}}}G^{(2)}(\bar{x}^{(2)},t), \quad x = \lambda - \mathrm{e}^{-2\sigma t^{\frac{1}{2}}}\bar{x}^{(2)}. \tag{58}$$

We have again omitted the bracketed superscripts in equations (57). At leading order, equations (57) become

$$F_{0_{\bar{x}\bar{x}}} = F_0 G_0^2, \quad \sigma(\bar{x}G_{0_{\bar{x}}} + G_0) = F_0 G_0^2, \tag{59a, b}$$

where $F(\bar{x},t) = F_0(\bar{x}) + o(1)$ and $G(\bar{x},t) = G_0(\bar{x}) + o(1)$, as $t \to \infty$. To match with the solution in region I(*b*), where $\alpha_- = o(1)$ and $\beta = O(1)$, we require that

$$F_0(\bar{x}) = o(\bar{x}\ln\bar{x}), \quad G_0(\bar{x}) = O(\bar{x}^{-1}) \quad \text{as} \quad \bar{x} \to \infty. \tag{60a, b}$$

Also, on using (58), we find that

$$A(t) \sim A_\infty^{(2)}\, t^{-\frac{1}{2}}\,\mathrm{e}^{-2\sigma t^{\frac{1}{2}}}, \tag{61}$$

for some positive constant $A_\infty^{(2)}$. The connection condition (13*a*) then requires that

$$F_0(0) = A_\infty, \tag{62a}$$

(omitting the bracketed superscript) and condition (13*b*) reduces, via (20) and (58), to

$$F_{0_{\bar{x}}}(0) = -1/\sqrt{\pi}. \tag{62b}$$

Equation (10b) shows that, as $x \to \lambda^-$, $\beta(x,t)$ has the same degree of smoothness as the initial input function, $g(x)$, for all $t \geqslant 0$. In particular, from equation (8d), $\beta(x,t) = 0((\lambda - x)\,p)$ as $x \to \lambda^-$, and hence

$$G_0(\bar{x}) = 0(\bar{x}p) \quad \text{as} \quad \bar{x} \to 0. \tag{63}$$

We also note that, since $\beta(\lambda,t) \to \infty$ as $t \to \infty$ when $p = 0$, equation (10b) shows that

$$\int_0^\infty A(t)\,\mathrm{d}t = \frac{1}{\beta_0\, g(\lambda)}, \quad \text{for} \quad p = 0. \tag{64}$$

To solve equations (59), it is convenient to subtract equation (59a) from (59b) and integrate once to obtain

$$F_{0_{\bar{x}}} = \sigma \bar{x} G_0 - 1/\sqrt{\pi}, \tag{65}$$

via conditions (62b) and (63). By defining new variables as

$$\hat{F}_0 = \bar{x}^{-1} F_0, \quad \hat{G}_0 = \bar{x} G_0, \quad \bar{x} = \mathrm{e}^s, \tag{66}$$

equations (59b) and (65) are reduced to the second order autonomous system

$$\hat{F}_{0_s} = \sigma \hat{G}_0 - \hat{F}_0 - 1/\sqrt{\pi}, \quad \sigma \hat{G}_{0_s} = \hat{F}_0\, \hat{G}_0^2. \tag{67a, b}$$

We require a solution of equations (67) subject to boundary conditions (60), (62) and (63), which become

$$\hat{F}_0(s) = o(s), \quad \hat{G}_0(s) = O(1) \quad \text{as} \quad s \to \infty, \tag{68a, b}$$

$$\hat{F}_0(s) \sim A_\infty\, \mathrm{e}^{-s}, \quad \hat{F}_{0_s}(s) + \hat{F}_0(s) \sim -1/\sqrt{\pi}, \quad \hat{G}_0(s) = O(\mathrm{e}^{(p+1)s}) \quad \text{as} \quad s \to -\infty. \tag{69a–c}$$

The system of equations (67) has two finite equilibrium points at $(0, 1/\sigma\sqrt{\pi})$ and $(-1/\sqrt{\pi}, 0)$ in the $(\hat{F}_0, \hat{G}_0)$ phase plane. The point $(0, 1/\sigma\sqrt{\pi})$ is a saddle with eigenvalues and associated eigenvectors given by

$$\rho_1 = -\tfrac{1}{2}\{1 + \sqrt{(1 + 4/\sigma^2\pi)}\}, \quad \boldsymbol{e}_{\rho_1} = (\rho_1, 1/\sigma^3\pi)^{\mathrm{T}}, \tag{70a}$$

$$\rho_2 = \tfrac{1}{2}\{-1 + \sqrt{(1 + 4/\sigma^2\pi)}\}, \quad \boldsymbol{e}_{\rho_2} = (\rho_2, 1/\sigma^3\pi)^{\mathrm{T}}. \tag{70b}$$

We do not need to analyse the form of the other equilibrium point, $(-1/\sqrt{\pi}, 0)$, since this lies outside the first quadrant of the $(\hat{F}_0, \hat{G}_0)$ phase plane, and we require a solution with $F_0 \geqslant 0$ and $G_0 \geqslant 0$ for $-\infty < s < \infty$. The phase portrait of the system of equations (67) is sketched in figure 14, where the stable separatrix of the point $(0, 1/\sigma\sqrt{\pi})$ is labelled as S_2. The unique integral path which satisfies conditions (68) as $s \to \infty$ is S_2, since $(0, 1/\sigma\sqrt{\pi})$ is the only equilibrium point in the first quadrant of the $(\hat{F}_0, \hat{G}_0)$ phase plane. Equations (67a, b) show that on S_2, $\hat{G}_0(s) \to 0$ and $\hat{F}_0(s) \to \infty$ as $s \to -\infty$. The behaviour of $\hat{F}_0$ and $\hat{G}_0$ is then readily obtained from equations (67a, b) and conditions (69a, b) as

$$\hat{F}_0(s) \sim A_\infty\, \mathrm{e}^{-s} - 1/\sqrt{\pi}, \quad \hat{G}_0(s) \sim B_\infty\, \mathrm{e}^s \quad \text{as} \quad s \to -\infty, \tag{71a, b}$$

where $B_\infty = \sigma/A_\infty$. The integral path S_2 thus satisfies condition (69c) only if $p = 0$. Therefore the boundary value problem (67), (68), (69) has a solution (which is unique) if and only if $p = 0$, and we conclude that, for $p = 1, 2, \ldots$, the asymptotic structure given by (21), (22) is not appropriate. At the end of this section we discuss the behaviour of solutions of the full initial-value problem with $g(x)$ continuous. When

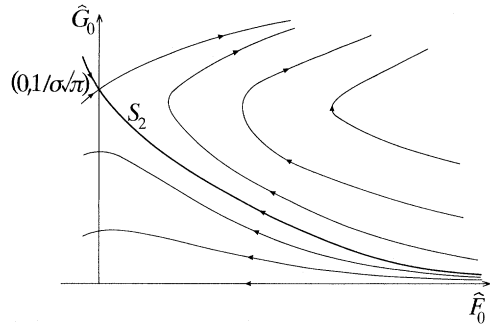

Figure 14. A sketch of the phase portrait of the system of equations (67).

the function $g(x)$ is discontinuous at $x=\lambda$, the solution is uniquely determined in terms of the constants A_∞ and σ, and has the asymptotic properties

$$\hat{F}_0(s) \sim -E(A_\infty,\sigma)\,\rho_1\,\mathrm{e}^{\rho_1 s}, \quad \hat{G}_0(s) \sim \frac{1}{\sigma\sqrt{\pi}} - E(A_\infty,\sigma)\,\frac{1}{\sigma^3\pi}\,\mathrm{e}^{\rho_1 s} \quad \text{as} \quad s\to\infty, \tag{72a, b}$$

with the behaviour as $s\to-\infty$ given in (71). Here E is fixed in terms of A_∞ and σ. On using (72) and (71) in (58), we find that

$$\alpha_- \sim -t^{-\frac{1}{2}}\mathrm{e}^{-2\sigma t^{\frac{1}{2}}}E(A_\infty,\sigma)\,\rho_1\,\bar{x}^{\rho_1+1}, \tag{73a}$$

$$\beta \sim \mathrm{e}^{2\sigma t^{\frac{1}{2}}}\{(1/\bar{x}\sigma\sqrt{\pi}) - E(A_\infty,\sigma)\,(1/\sigma^3\pi)\,\bar{x}^{\rho_1-1}\}, \quad \text{with } \bar{x}\gg 1 \quad \text{as} \quad t\to\infty, \tag{73b}$$

$$\alpha_- \sim t^{-\frac{1}{2}}\mathrm{e}^{-2\sigma t^{\frac{1}{2}}}\{A_\infty - \bar{x}/\sqrt{\pi}\}, \tag{74a}$$

$$\beta \sim B_\infty\,\mathrm{e}^{2\sigma t^{\frac{1}{2}}}, \quad \text{with} \quad \bar{x}\ll 1 \quad \text{as} \quad t\to\infty. \tag{74b}$$

Approximations (74) remain uniform as $\bar{x}\to 0$. The approximation (73b), however, becomes non-uniform when $\bar{x}=O(\mathrm{e}^{2\sigma t^{\frac{1}{2}}})$, or $(\lambda-x)=O(1)$ and we move into region I(b). In region I(b), approximations (73) demonstrate that $\alpha_-(x,t)=O(t^{-\frac{1}{2}}\mathrm{e}^{2\rho_1\sigma t^{\frac{1}{2}}})$ and $\beta=O(1)+O(\mathrm{e}^{2\rho_1\sigma t^{\frac{1}{2}}})$. Appropriate scaled variables in region I(b) are therefore

$$\alpha_-(x,t) = t^{-\frac{1}{2}}\mathrm{e}^{2\rho_1\sigma t^{\frac{1}{2}}}\gamma^{(2)}(x,t), \quad \beta(x,t) = \beta_\infty^{(2)}(x) + \mathrm{e}^{2\rho_1\sigma t^{\frac{1}{2}}}\theta^{(2)}(x,t). \tag{75a, b}$$

In terms of these scaled variables, equations (12a, b) become, at leading order

$$\gamma_{0_{xx}} = \beta_\infty^2\,\gamma_0, \quad \rho_1\,\sigma\theta_0 = \beta_\infty^2\,\gamma_0, \tag{76a, b}$$

where $\gamma^{(2)}(x,t)=\gamma_0(x)+o(1)$ and $\theta^{(2)}(x,t)=\theta_0(x)+o(1)$ as $t\to\infty$. Matching with region I(a) leads to the boundary conditions

$$\left.\begin{aligned} \gamma_0(x) &\sim -E(A_\infty,\sigma)\,\rho_1(\lambda-x)^{\rho_1+1}, && (77a)\\ \theta_0(x) &\sim -E(A_\infty,\sigma)\,(\lambda-x)^{\rho_1-1}/\sigma^3\pi, && (77b)\\ \beta_\infty(x) &\sim \{\sigma\sqrt{\pi}(\lambda-x)\}^{-1}, && (77c) \end{aligned}\right\} \quad \text{as} \quad x\to\lambda^-,$$

whilst condition (12d) requires that

$$(\mathrm{d}\gamma_0/\mathrm{d}x)\,(0) = (\mathrm{d}\theta_0/\mathrm{d}x)\,(0) = 0. \tag{78}$$

The function $\beta_\infty(x)$ cannot be determined by the asymptotic analysis as $t\to\infty$ and depends upon the specific form of the initial input function, $\beta_0\,g(x)$. However,

equations (76) and boundary conditions (77a, b), (78) determine $\gamma_0(x)$ and $\theta_0(x)$ uniquely for any strictly positive function $\beta_\infty(x)$ which satisfies condition (77c) with $\beta'_\infty(0) = 0$.

The leading order solution thus depends upon the two strictly positive constants A_∞ and σ, which are not determined by the above analysis. It is of interest to examine whether these constants are fixed at higher order in the large time-asymptotic development or remain undetermined to all orders. This is discussed in Billingham (1991), where it is shown that σ and A_∞ remain undetermined to all orders in the asymptotic expansions as $t \to \infty$. This is perhaps not too unexpected as the governing equations (7a, b) are parabolic. The same situation arises in boundary-layer theory (where the governing equations are also parabolic), and is resolved by Stewartson (1957). We expect that the same general remarks made in that paper will apply here, as they are consequences of the parabolic nature of boundary-layer problems.

In summary, we note that the large time-asymptotic structure (23) is only possible in cubic autocatalysis when $p = 0$, i.e. when $g(x)$ is discontinuous at $x = \lambda$. In this case, we have that in region I(a), $0 \leqslant (\lambda - x) = O(\mathrm{e}^{-2\sigma t^{\frac{1}{2}}})$ and

$$\alpha_- = t^{-\frac{1}{2}}\mathrm{e}^{-2\sigma t^{\frac{1}{2}}}F_0(\bar{x}) + o(t^{-\frac{1}{2}}\mathrm{e}^{-2\sigma t^{\frac{1}{2}}}), \quad \beta = \mathrm{e}^{2\sigma t^{\frac{1}{2}}}G_0(\bar{x}) + o(\mathrm{e}^{2\sigma t^{\frac{1}{2}}}), \tag{79a, b}$$

where the functions F_0 and G_0 are the unique solutions of the boundary value problem, (59), (60), (62), (63). As an illustration, we calculate the functions $F_0(\bar{x})$ and $G_0(\bar{x})$ numerically in the case $A_\infty = 1$, $\sigma = 1$. We integrate equations (67) using a fourth order Runge–Kutta method and find that $E(1, 1) \approx 0.606$. The functions $F_0(\bar{x})$ and $G_0(\bar{x})$ are plotted in figure 15. Figure 9 shows a typical solution of the full initial value problem, where the concentration β has a similar functional form in region I(a) to that exhibited by $G_0(\bar{x})$. In region I(b), $0 < (\lambda - x) = O(1)$, and

$$\alpha_- \sim t^{-\frac{1}{2}}\mathrm{e}^{2\rho_1\sigma t^{\frac{1}{2}}}\gamma_0(x), \quad \beta \sim \beta_\infty(x) + \mathrm{e}^{2\rho_1\sigma t^{\frac{1}{2}}}\theta_0(x), \tag{80a, b}$$

where the functions $\gamma_0(x)$ and $\theta_0(x)$ are the unique solutions of the boundary-value problem (76), (77), (78), and the positive function $\beta_\infty(x)$ satisfies condition (77c). The solution in region I(b) thus depends upon the initial conditions (12c) through the unknown function $\beta_\infty(x)$. Finally, via (61), we have that

$$\alpha_+ \sim \operatorname{erf}(\tfrac{1}{2}\eta) + O(t^{-\frac{1}{2}}\mathrm{e}^{-2\sigma t^{-\frac{1}{2}}}) \quad \text{as} \quad t \to \infty \quad \text{for} \quad x > \lambda, \tag{80c}$$

where $\eta = (x - \lambda)\, t^{-\frac{1}{2}}$.

We now turn our attention to the behaviour of solutions of the initial value problem when $p = 1, 2, \ldots$ under cubic autocatalysis. The numerical solutions which we described in §2 indicate that $\alpha(x_0, t) = O(t^{-\frac{1}{2}})$ as $t \to \infty$ for x_0 in the neighbourhood of the point $x = \lambda$, and expression (10b) then shows that $\beta(x_0, t) \to \infty$ as $t \to t^*$ for some finite $t^* > 0$. However, we do not expect that finite time blow up in the concentration β occurs in this case, since such behaviour does not arise when $p = 0$ and the rate of growth of β is much greater than for $p = 1, 2, \ldots$. We conclude that in fact $\alpha(x_0, t) = o(t^{-\frac{1}{2}})$ as $t \to \infty$ and that the spike in β approaches the point $x = \lambda$ so that $x_{\max}(t) \to \lambda$ as $t \to \infty$. From the numerical results illustrated in figures 10a, b and 11 b, $x_{\max}(t) \to \lambda$ extremely slowly as $t \to \infty$. We have demonstrated above that no asymptotic solution with the structure (58) is available for $p = 1, 2, \ldots$, and conclude that the form of the solution as $t \to \infty$ is entirely different in this case and remains to be determined. This is not pursued further in the present paper.

It may also be possible for solutions under quadratic autocatalysis to behave in a

PHILOSOPHICAL TRANSACTIONS OF THE ROYAL SOCIETY A MATHEMATICAL, PHYSICAL & ENGINEERING SCIENCES

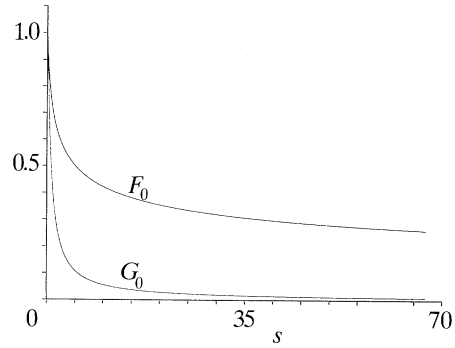

Figure 15. A graph of the function $F_0(\bar{x})$ and $G_0(\bar{x})$, calculated from the numerical solution of equations (103) when $A_\infty = 1$ and $\sigma = 1$.

similar manner to solutions under cubic autocatalysis with $p = 1, 2, \ldots$. We have shown that an asymptotic solution of equations (11), (12), (13) with $n = 1$, based on the structure (20) requires $g(x) = O((\lambda - x)^p)$ as $x \to \lambda^-$. However, if all the derivatives of $g(x)$ vanish at $x = \lambda$ (for example, $g(x) = O(\mathrm{e}^{-1/(\lambda - x)})$ as $x \to \lambda^-$) this asymptotic solution is not available. Although this type of input function cannot be modelled accurately by our numerical method, we expect that a spike in β will again form but not in the immediate neighbourhood of $x = \lambda$, and behave in a qualitatively similar manner to that found for cubic autocatalysis with $p = 1, 2, \ldots$. We conjecture that, for $n = 1, 2$, any bounded, continuous positive input function $g(x)$ is a member of one of two classes of functions $P^{(n)}$ and $Q^{(n)}$. If $g(x) \in P^{(n)}$ then the solution of the initial value problem (11), (12), (13) develops a spike in β in the immediate neighbourhood of the point $x = \lambda$ and possesses the asymptotic structure (20) whilst if $g(x) \in Q^{(n)}$ the solution develops a spike in β which drifts extremely slowly towards the point $x = \lambda$. We have determined $P^{(2)}$ and $Q^{(2)}$ as

$$P^{(2)} = \{g(x) : g(\lambda) > 0\}, \quad Q^{(2)} = \{g(x) : g(\lambda) = 0\}, \tag{81a}$$

and postulate that $P^{(1)}$ and $Q^{(1)}$ are defined by

$$\left.\begin{aligned} P^{(1)} &= \{g(x) : g(x) = O((\lambda - x)^p) \text{ as } x \to \lambda^-, \text{ for } p \geqslant 0\}, \\ Q^{(1)} &= \{g(x) : g(x) = o((\lambda - x)^p) \text{ as } x \to \lambda^-, \text{ for } \forall\, p \geqslant 0\}, \end{aligned}\right\} \tag{81b}$$

To conclude, we emphasize two interesting features of the solution when $D = 0$. First, the definitions (81) of the classes of functions $Q^{(1)}$ and $Q^{(2)}$ show that $Q^{(2)}$ is 'larger' than $Q^{(1)}$ in the sense that $Q^{(1)} \subset Q^{(2)}$. A function $g(x)$ is a member of $Q^{(n)}$ if the corresponding rate of reaction in the neighbourhood of the point $x = \lambda$ is too small to generate a spike in β and set up the asymptotic structure (23) as $t \to \infty$. Clearly, this criterion is satisfied by a larger set of functions $g(x)$ under cubic autocatalysis than under quadratic autocatalysis, since the rate of reaction is of $O(\alpha\beta^n)$. Second, the spike in β grows algebraically in each of the above cases, except for $n = 2$ and $g(x) \in P^{(2)}$, when the spike grows exponentially. In other words, when the initial input of the autocatalyst, B, is discontinuous under cubic autocatalysis the reaction proceeds much more rapidly and the spike in β becomes much larger and narrower than in any other case.

In the next section we use the results which we have obtained here for the case

$D = 0$ to obtain the full asymptotic development of the initial value problem (7), (8) in $x, t \geqslant 0$ for $0 < D \ll 1$.

4. The solution of the full initial-value problem with $0 < D \ll 1$

We now consider the solution of the full initial-value problem, (7), (8), with $0 < D \ll 1$ and explain the features which we described in §2. We expand α and β as

$$\alpha(x,t) = \hat{\alpha}_0(x,t) + o(1), \quad \beta(x,t) = \hat{\beta}_0(x,t) + o(1) \quad \text{as} \quad D \to 0. \tag{82}$$

On substituting these expansions into equations (7), we obtain, at leading order in D, the initial-value problem (11), (12), (13) for $\hat{\alpha}_0, \hat{\beta}_0$ which we analysed in §3. The solution of this initial-value problem has $\hat{\beta}_0$ identically zero in $x > \lambda$, but non-zero in $0 \leqslant x \leqslant \lambda$. This leads to a singularity in sufficiently large x-derivatives of $\hat{\beta}_0$ at $x = \lambda$ for all $t \geqslant 0$, with the order of the singularity depending upon the value of $p = 0, 1, 2, \ldots$. However, solutions of the full initial-value problem (7), (8), in which the term $D\beta_{xx}$ is retained, must be analytic across $x = \lambda$. We conclude that expansions of the type (82) are non-uniform as $x \to \lambda$ for all $t > 0$. Physically, this non-uniformity arises from the slow diffusion of β into $x > \lambda$. To describe the development in the neighbourhood of the point $x = \lambda$, a further region must be introduced in which the term $D\beta_{xx}$ is retained at leading order. By considering equation (7*b*), we find that this region has width of $O(D^{\frac{1}{2}})$ as $D \to 0$. In this region $\alpha = O(1)$ and $\beta = O(D^{\frac{1}{2}p})$, from condition (8*d*). There are, therefore, three asymptotic regions to be considered when $t = O(1)$. From equations (7), we can summarize the problem in each region as:

Region I; $0 \leqslant x < \lambda - O(D^{\frac{1}{2}}), \quad t = O(1)$

$$\alpha = \alpha_{\mathrm{I}}(x,t) + o(1), \quad \beta = \beta_{\mathrm{I}}(x,t) + o(1) \quad \text{as} \quad D \to 0, \tag{82a, b}$$

where

$$\partial\alpha_{\mathrm{I}}/\partial t = \partial^2\alpha_{\mathrm{I}}/\partial x^2 - \alpha_{\mathrm{I}}\beta_{\mathrm{I}}^n, \quad \partial\beta_{\mathrm{I}}/\partial t = \alpha_{\mathrm{I}}\beta_{\mathrm{I}}^n, \quad 0 \leqslant x < \lambda, \quad t \geqslant 0. \tag{83a, b}$$

Region II; $X = D^{-\frac{1}{2}}(x - \lambda) = O(1), \quad t = O(1)$

$$\alpha = \alpha_{\mathrm{II}}(X,t) + o(1), \quad \beta = D^{\frac{1}{2}p}\beta_{\mathrm{II}}(X,t) + o(D^{\frac{1}{2}p}) \quad \text{as} \quad D \to 0,$$

where

$$\frac{\partial^2\alpha_{\mathrm{II}}}{\partial X^2} = 0, \quad \frac{\partial\beta_{\mathrm{II}}}{\partial t} = \begin{cases} \partial^2\beta_{\mathrm{II}}/\partial X^2 + \alpha_{\mathrm{II}}\beta_{\mathrm{II}}^n, & n = 1 \quad \text{or} \quad p = 0, \\ \partial^2\beta_{\mathrm{II}}/\partial X^2, & n = 2, \quad p = 1, 2, \ldots, \end{cases} \tag{84a–c}$$

with $-\infty < X < \infty$, $t \geqslant 0$.

Region III; $x > \lambda + O(D^{\frac{1}{2}})$, $t = O(1)$

$$\alpha = \alpha_{\mathrm{III}}(x,t) + o(1), \quad \beta = D^{p+\frac{1}{2}} \exp\{-(\psi_0(x,t)/D) + o(D^{-1})\}, \quad \text{as} \quad D \to 0,$$

where

$$\partial\alpha_{\mathrm{III}}/\partial t = \partial^2\alpha_{\mathrm{III}}/\partial x^2, \quad \partial\psi_0/\partial t + (\partial\psi_0/\partial x)^2 = 0, \quad x > \lambda, \quad t \geqslant 0. \tag{85a, b}$$

Equations (83) are to be solved subject to boundary conditions (8*b*) and matching with the solution in region II, equations (84) subject to matching with the solutions in regions I and III, and equations (85) subject to boundary conditions (8*c*) and matching with the solution in region II. The initial conditions for equations (83)–(85) are given by (8*a*).

We begin in region II, where equation (84*a*) shows that α_{II} is linear in the variable X. However, to match the function $\alpha_{II}(X,t)$ with $\alpha_I = O(1)$ in region I and $\alpha_{III} = O(1)$ in region III, α_{II} must be a function of t alone. It is then clear that the leading order solutions in regions I and III (up to exponentially small terms in D) are given by the solutions of the initial-value problem (11)–(13), that is

$$\alpha_I(x,t) \equiv \alpha_-(x,t), \quad \alpha_{III}(x,t) \equiv \alpha_+(x,t), \quad \beta_I(x,t) \equiv \beta(x,t)$$

and then, from §3

$$\alpha_{II}(X,t) \equiv A(t) \quad \forall\, |X| \geqslant 0, \quad t \geqslant 0. \tag{86}$$

We consider the cases of quadratic and cubic autocatalysis separately.

(*a*) *Quadratic autocatalysis*, $n = 1$

We continue in region II, and consider first the case when $p = 0$. Equations (84*b*) and (86) lead to

$$\partial\beta_{II}/\partial t = \partial^2\beta_{II}/\partial X^2 + A(t)\beta_{II}, \quad -\infty < X < \infty, \quad t > 0 \tag{87a}$$

whilst the initial conditions are, via (8*d*)

$$\beta_{II}(X,0) = \begin{cases} 0, & X > 0, \\ \beta_0 g_\lambda, & X < 0, \end{cases} \tag{87b}$$

and matching to regions I and III requires

$$\beta_{II}(X,t) \to 0 \quad \text{as} \quad X \to \infty, \quad t \geqslant 0, \tag{87c}$$

$$\beta_{II}(X,t) \to \beta_0 g_\lambda \exp\left[\int_0^t A(\tau)\,\mathrm{d}\tau\right] \quad \text{as} \quad X \to -\infty, \quad t \geqslant 0. \tag{87d}$$

The initial condition (87*b*) suggests that we should introduce the similarity variable $\bar\eta = Xt^{-\frac{1}{2}}$, in terms of which equation (87*a*) becomes

$$\partial^2\beta_{II}/\partial\bar\eta^2 + \tfrac{1}{2}\bar\eta\,\partial\beta_{II}/\partial\bar\eta = t\{\partial\beta_{II}/\partial t - A(t)\,\beta_{II}\}, \quad -\infty < \bar\eta < \infty, \quad t \geqslant 0. \tag{88a}$$

We observe that the function

$$\beta_0 g_\lambda \exp\left[\int_0^t A(\tau)\,\mathrm{d}\tau\right]$$

satisfies identically the right-hand side of equation (88*a*), which suggests that we try a solution in the form

$$\beta_{II}(\bar\eta,t) = \beta_0 g_\lambda \exp\left[\int_0^t A(\tau)\,\mathrm{d}\tau\right] U(\bar\eta). \tag{88b}$$

The resulting problem for $U(\bar\eta)$ is then

$$U'' + \tfrac{1}{2}\bar\eta U' = 0; \quad -\infty < \bar\eta < \infty, \quad U(\bar\eta) \to \begin{cases} 0, & \bar\eta \to \infty, \\ 1, & \bar\eta \to -\infty. \end{cases}$$

The solution of this problem is readily obtained as $U(\bar\eta) = \frac{1}{2}[1 - \mathrm{erf}\,(\frac{1}{2}\bar\eta)]$, and we then have

$$\beta_{II}(\bar\eta,t) = \tfrac{1}{2}\beta_0 g_\lambda \exp\left[\int_0^t A(\tau)\,\mathrm{d}\tau\right][1 - \mathrm{erf}\,(\tfrac{1}{2}\bar\eta)], \quad -\infty < \bar\eta < \infty, \quad t > 0. \tag{89}$$

Therefore, in region II, when $p = 0$

$$\alpha_{\mathrm{II}} \sim A(t), \tag{90a}$$

$$\beta_{\mathrm{II}} \sim \tfrac{1}{2}\beta_0 g_\lambda \exp\left[\int_0^t A(\tau)\,\mathrm{d}\tau\right]\left[1-\mathrm{erf}\left\{\frac{(x-\lambda)}{2(Dt)^{\frac{1}{2}}}\right\}\right] \quad \text{as} \quad D\to 0. \tag{90b}$$

By comparing the asymptotic solution in regions I, II and III with the solution of the initial-value problem (11), (12), (13) when $D = 0$, we see that, at leading order, the only difference is that for $0 < D \ll 1$, the initial discontinuity in β is smoothed out by diffusion over a region with width of $O(D^{\frac{1}{2}}t^{\frac{1}{2}})$. This behaviour can be clearly seen in the numerical solution of the initial value problem during the first induction phase, illustrated in figure 1*c*.

When $p = 1, 2, \ldots$, equation (10*a*), together with conditions (12*b*) and (8*d*) lead us to replace the matching condition (87*d*) with

$$\beta_{\mathrm{II}}(X,t) \sim \beta_0 g_\lambda (-X)^p \exp\left[\int_0^t A(\tau)\,\mathrm{d}\tau\right] \quad \text{as} \quad X\to-\infty, \tag{91a}$$

and initial conditions (87*b*) with

$$\beta_{\mathrm{II}}(X,0) = \begin{cases} 0, & X \geqslant 0, \\ \beta_0 g_\lambda (-X)^p, & X < 0, \end{cases} \tag{91b}$$

whilst the matching condition (87*c*) remains the same. We again introduce the variable $\bar{\eta}$, and look for a solution of equation (88*a*) in the form

$$\beta_{\mathrm{II}} = t^{\frac{1}{2}p} \exp\left[\int_0^t A(\tau)\,\mathrm{d}\tau\right]\omega(\bar{\eta}).$$

The equation for $\omega(\bar{\eta})$ is then

$$\omega'' + \tfrac{1}{2}\bar{\eta}\omega' - \tfrac{1}{2}p\omega = 0, \quad -\infty < \bar{\eta} < \infty, \tag{92a}$$

which, to satisfy the conditions (91*a*, *b*), (87*c*), must be solved subject to

$$\omega(\bar{\eta}) \to \begin{cases} 0, & \bar{\eta}\to\infty, \\ \beta_0 g_\lambda (-\bar{\eta})^p, & \bar{\eta}\to-\infty. \end{cases} \tag{92b}$$

The solution to equation (92*a*) subject to conditions (92*b*) is obtained in Billingham (1991) as

$$\omega(\bar{\eta}) = \begin{cases} k_0 \tilde{A}(\bar{\eta}) \displaystyle\int_{\bar{\eta}}^{\infty} \frac{\mathrm{e}^{-\frac{1}{4}s^2}}{\tilde{A}^2(s)}\,\mathrm{d}s, & \bar{\eta} \geqslant 0, \qquad (93a) \\ k_1 \tilde{A}(\bar{\eta}) \displaystyle\int_{-\infty}^{\bar{\eta}} \frac{\mathrm{e}^{-\frac{1}{4}s^2}}{\tilde{A}^2(s)}\,\mathrm{d}s + k_2 \tilde{A}(\bar{\eta}), & \bar{\eta} \leqslant 0, \qquad (93b) \end{cases}$$

where

$$\tilde{A}(\bar{\eta}) = \begin{cases} \displaystyle\sum_{r=0}^{\frac{1}{2}p} \frac{(\frac{1}{2}p)!\,\bar{\eta}^{2r}}{(2r)!\,(\frac{1}{2}p-r)!}, & p \text{ even}, \qquad (93c) \\ \displaystyle\sum_{r=0}^{\frac{1}{2}(p-1)} \frac{\{\frac{1}{2}(p-1)\}!\,\bar{\eta}^{2r+1}}{(2r+1)!\,\{\frac{1}{2}(p-1)-r\}!}, & p \text{ odd}, \qquad (93d) \end{cases}$$

and

$$k_0 = -k_1 = \begin{cases} \dfrac{\beta_0 g_\lambda p!}{2K(\frac{1}{2}p)!}, & p \text{ even}, \quad (94a) \\ \dfrac{\beta_0 g_\lambda p!}{2\bar{K}\{\frac{1}{2}(p-1)\}!}, & p \text{ odd}, \quad (94b) \end{cases}$$

$$k_2 = \begin{cases} \dfrac{\beta_0 g_\lambda p!}{(\frac{1}{2}p)!}, & p \text{ even}, \quad (94c) \\ -\dfrac{\beta_0 g_\lambda p!}{\{\frac{1}{2}(p-1)\}!}, & p \text{ odd}. \quad (94d) \end{cases}$$

Here, the positive constants K and $\bar{K}$ are defined by the improper integrals

$$K = \int_0^\infty \frac{\mathrm{e}^{-\frac{1}{4}s^2}}{\tilde{A}^2(s)}\,\mathrm{d}s = \frac{p!\sqrt{\pi}}{2^p\{(\frac{1}{2}p)!\}^2}, \quad p \text{ even}, \quad (94e)$$

$$\bar{K} = \int_0^\infty \left\{\frac{1}{s^2} - \frac{\mathrm{e}^{-\frac{1}{4}s^2}}{\tilde{A}^2(s)}\right\}\mathrm{d}s, \quad p \text{ odd}. \quad (94f)$$

This solution, which satisfies conditions (92*b*), indicates that diffusion again acts over a region with thickness of $O(D^{\frac{1}{2}}t^{\frac{1}{2}})$. In this case, the only noticeable effect is a slow leakage of the autocatalyst, B, into the region $x > \lambda$.

It remains to determine the first term ψ_0 in the exponentially small WKBJ type expansion for β in region III. The equation (85*b*) must be solved subject to the matching, boundary and initial conditions

$$\psi_0(x,t) \to \infty \quad \text{as} \quad t \to 0 \quad \forall\, x > \lambda \quad \text{and as} \quad x \to \infty \quad \forall\, t > 0, \quad (95a, b)$$

$$\psi_0(x,t) \sim (x-\lambda)^2/4t \quad \text{as} \quad x \to \lambda^+ \quad \forall\, t > 0. \quad (95c)$$

The matching condition (95*c*) is obtained via (90*b*) when $p = 0$, or (93*a*) when $p = 1, 2, \ldots$. The solution of equation (85*b*) subject to (95*a*–*c*) is readily obtained as

$$\psi_0(x,t) = (x-\lambda)^2/4t; \quad x > \lambda, \quad t > 0, \quad (95d)$$

which gives an exponentially small, weakly diffusing layer of β in region III.

The expansions in regions I, II, III provide a uniform approximation to the solution of the full initial-value problem (7), (8) for all $x \geqslant 0$ and $t = 0(1)$ as $D \to 0$. It remains to see whether these expansions remain uniform as $t \to \infty$. This can be investigated directly, as we have obtained the complete solution to the leading order problem in II, and the large time-asymptotic development of the leading order problems in I and III (see §3).

An examination of the long-time asymptotic development in regions I and II shows that a non-uniformity first develops in the neighbourhood of $x = \lambda$ as $t \to \infty$. The leading order solutions $\alpha_{\mathrm{I}}, \beta_{\mathrm{I}}$ in region I develop a thin layer close to $x = \lambda^-$ of thickness $O(t^{-\frac{1}{2}})$, in which the self-similar spike in β_{I} emerges. However, the leading order solutions (90), (93) show that region II thickens about $x = \lambda$ as $t \to \infty$, with thickness of $O(D^{\frac{1}{2}}t^{\frac{1}{2}})$. When the width of region II becomes comparable with the width of the self-similar structure in region I, matching between regions I and II fails, and a non-uniformity occurs. The timescale for this non-uniformity to develop is when

$t^{-\frac{1}{2}} = O(D^{\frac{1}{2}}t^{\frac{1}{2}})$ which gives $t = O(D^{-1})$. The length scale over which the non-uniformity occurs is thus $x = \lambda + O(D^{\frac{1}{4}})$ with $\alpha = O(D^{\frac{1}{2}})$ and $\beta = O(D^{-\frac{1}{2}})$ (estimates obtained from the long time development in region II or region I as $x \to \lambda^-$). We identify the development of this non-uniformity with the end of the first induction phase, and the above order estimates (in particular $\beta_{\max}(t_1) = O(D^{-\frac{1}{2}})$, $t_1 = O(D^{-\frac{1}{2}})$) are in good agreement with the numerical results given in table 1.

To continue the asymptotic solution of the full initial-value problem (7), (8) as $D \to 0$ into times $t = O(D^{-\frac{1}{2}})$ and beyond, we must introduce further regions to accommodate the local non-uniformity developing near $x = \lambda$. The appropriate structure for $t = O(D^{-\frac{1}{2}})$ is readily deduced from the long-time asymptotics for $\alpha_{\rm I}, \beta_{\rm I}$ and $\alpha_{\rm III}, \beta_{\rm III}$ (in §3), together with the present analysis of the developing non-uniformity near $x = \lambda$. We require four regions, in which the complete leading order problems are as follows, with $\hat{t} = D^{\frac{1}{2}}t = O(1)$.

Region IV; $0 < x < \lambda - O(D^{\frac{1}{4}})$, $\hat{t} = O(1)$

$$\alpha = D^{\frac{1}{2}-\frac{1}{4}\mu_1}\alpha_{\rm IV}(x,\hat{t}) + o(D^{\frac{1}{2}-\frac{1}{4}\mu_1}), \quad \beta = \beta_{\rm IV}(x,\hat{t}) + o(1) \quad \text{as} \quad D \to 0,$$

where

$$\partial^2\alpha_{\rm IV}/\partial x^2 - \alpha_{\rm IV}\beta_{\rm IV} = 0, \quad \partial\beta_{\rm IV}/\partial\hat{t} = 0, \quad 0 \leqslant x < \lambda, \quad \hat{t} > 0, \tag{96a, b}$$

subject to the conditions

$$\alpha_{\rm IV}(x,\hat{t}) \sim \hat{t}^{\frac{1}{2}\mu_1 - 1}\gamma_0(x) \quad \text{as} \quad \hat{t} \to 0, \quad 0 \leqslant x < \lambda - O(D^{\frac{1}{4}}), \tag{96c}$$

$$\beta_{\rm IV}(x,\hat{t}) \to \beta_\infty(x) \quad \text{as} \quad \hat{t} \to 0, \quad 0 \leqslant x < \lambda - O(D^{\frac{1}{4}}), \tag{96d}$$

on matching to region I;

$$\alpha_{\rm IV}(x,\hat{t}) = O([\lambda - x]^{\mu_1}) \quad \text{as} \quad x \to \lambda^-, \quad \hat{t} = O(1), \tag{96e}$$

$$\beta_{\rm IV}(x,\hat{t}) = O([\lambda - x]^{-2}) \quad \text{as} \quad x \to \lambda^-, \quad \hat{t} = O(1), \tag{96f}$$

on matching to region V; and

$$\partial\beta_{\rm IV}/\partial x = \partial\alpha_{\rm IV}/\partial x = 0 \quad \text{at} \quad x = 0, \quad \hat{t} > 0. \tag{96g}$$

Region V; $\hat{X} = D^{-\frac{1}{4}}(x - \lambda) = O(1)$, $\hat{t} = O(1)$,

$$\alpha = D^{\frac{1}{2}}\alpha_{\rm V}(\hat{X},\hat{t}) + o(D^{\frac{1}{2}}), \quad \beta = D^{-\frac{1}{2}}\beta_{\rm V}(\hat{X},\hat{t}) + o(D^{-\frac{1}{2}}) \quad \text{as} \quad D \to 0,$$

where

$$\partial^2\alpha_{\rm V}/\partial\hat{X}^2 - \alpha_{\rm V}\beta_{\rm V} = 0, \quad \partial^2\beta_{\rm V}/\partial\hat{X}^2 + \alpha_{\rm V}\beta_{\rm V} = \partial\beta_{\rm V}/\partial\hat{t}, \quad -\infty < \hat{X} < \infty, \quad \hat{t} > 0, \tag{97a, b}$$

subject to the matching conditions

$$\alpha_{\rm V}(\hat{X},\hat{t}) \sim A_\infty/\hat{t} \quad \text{as} \quad \hat{t} \to 0, \quad -\infty < \hat{X} < \infty, \tag{97c}$$

$$\beta_{\rm V}(\hat{X},\hat{t}) \sim \begin{cases} \beta_0 g_\lambda \hat{t}[1 - \operatorname{erf}(\hat{X}/2\hat{t}^{\frac{1}{2}})], & p = 0, \\ \hat{t}^{(1+p)}\omega(\hat{X}/2\hat{t}^{\frac{1}{2}}), & p = 1, 2, \ldots, \end{cases} \quad \text{as} \quad \hat{t} \to 0, \quad -\infty < \hat{X} < \infty, \tag{97d}$$

on matching to II, I, III as $\hat{t} \to 0$ for all $|\hat{X}| \geqslant 0$;

$$\alpha_{\rm V}(\hat{X},\hat{t}) = O(\hat{X}^{\mu_1}), \quad \beta_{\rm V}(\hat{X},\hat{t}) = O(\hat{X}^{-2}) \quad \text{as} \quad \hat{X} \to -\infty, \quad \hat{t} > 0, \tag{97e, f}$$

PHILOSOPHICAL TRANSACTIONS OF THE ROYAL SOCIETY A MATHEMATICAL, PHYSICAL & ENGINEERING SCIENCES

on matching with region IV;

$$\alpha_{\rm V}(\hat{X},\hat{t}) \sim \hat{X}/(\pi\hat{t})^{\frac{1}{2}}, \quad \beta_{\rm V}(\hat{X},\hat{t}) = O(\mathrm{e}^{-\hat{X}^2/4\hat{t}}), \quad \text{as} \quad \hat{X}\to\infty, \quad \hat{t}>0, \qquad (97g,h)$$

on matching with region VI(*a*).

Region VI(*a*); $x = \lambda + O(1), \quad \hat{t} = O(1)$

$$\alpha = D^{\frac{1}{4}}\tilde{\alpha}_{\rm VI}(x,\hat{t}) + o(D^{\frac{1}{4}}), \quad \beta = D^{p+\frac{1}{2}}\exp\{-\tilde{\psi}_0(x,\hat{t})/D^{\frac{1}{2}} + o(D^{-\frac{1}{2}})\} \quad \text{as} \quad D\to 0,$$

where

$$\partial^2\alpha_{\rm VI}/\partial x^2 = 0, \quad \partial\tilde{\psi}_0/\partial\hat{t} + (\partial\tilde{\psi}_0/\partial x)^2 = 0, \quad x>\lambda, \quad \hat{t}>0, \qquad (98a,b)$$

subject to the matching conditions

$$\tilde{\alpha}_{\rm VI}(x,\hat{t}) \sim (x-\lambda)/(\pi\hat{t})^{\frac{1}{2}}, \quad \tilde{\psi}_0(x,\hat{t}) \sim (x-\lambda)^2/4\hat{t} \quad \text{as} \quad \hat{t}\to 0, \quad x>\lambda, \quad (98c,d)$$

on matching to region III;

$$\tilde{\alpha}_{\rm VI}(x,\hat{t})\to 0, \quad \tilde{\psi}_0(x,\hat{t})\to 0 \quad \text{as} \quad x\to\lambda, \quad \hat{t}>0, \qquad (98e,f)$$

on matching to region V;

$$\tilde{\alpha}_{\rm VI}(x,\hat{t}) = O(x), \quad \tilde{\psi}_0(x,\hat{t}) = O(x^2) \quad \text{as} \quad x\to\infty, \quad \hat{t}>0, \qquad (99a,b)$$

on matching to region VI(*b*).

Region VI(*b*); $\hat{x} = D^{\frac{1}{4}}(x-\lambda) = O(1), \hat{t} = O(1)$

$$\alpha = \hat{\alpha}_{\rm VI}(\hat{x},\hat{t}) + o(1), \quad \beta = D^{p+\frac{1}{2}}\exp\{-\hat{\psi}_0(\hat{x},\hat{t})/D + o(D^{-1})\} \quad \text{as} \quad D\to 0,$$

where

$$\partial\hat{\alpha}_{\rm VI}/\partial\hat{t} = \partial^2\hat{\alpha}_{\rm VI}/\partial\hat{x}^2, \quad \partial\hat{\psi}_0/\partial\hat{t} + (\partial\hat{\psi}_0/\partial\hat{x})^2 = 0, \quad \hat{x}>0, \quad \hat{t}>0 \qquad (100a,b)$$

subject to the matching conditions

$$\hat{\alpha}_{\rm VI}(\hat{x},\hat{t}) \sim \mathrm{erf}\,(\hat{x}/2\hat{t}^{\frac{1}{2}}) \quad \text{as} \quad \hat{t}\to 0, \quad \hat{x}>0, \qquad (100c)$$

$$\hat{\psi}_0(\hat{x},\hat{t}) \sim \hat{x}^2/4\hat{t} \quad \text{as} \quad \hat{t}\to 0, \quad \hat{x}>0, \qquad (100d)$$

on matching to region III;

$$\hat{\alpha}_{\rm VI}(\hat{x},\hat{t}) = O(\hat{x}), \quad \hat{\psi}_0(\hat{x},\hat{t}) = O(\hat{x}^2) \quad \text{as} \quad \hat{x}\to 0, \quad \hat{t}>0, \qquad (100e,f)$$

on matching to region VI(*a*), together with the original boundary conditions (8*c*)

$$\hat{\alpha}_{\rm VI}(\hat{x},\hat{t})\to 1, \quad \hat{\psi}_0(\hat{x},\hat{t})\to\infty \quad \text{as} \quad \hat{x}\to\infty, \quad \hat{t}>0. \qquad (100g,h)$$

The leading order problems in each of regions IV–VI(*b*) are well-posed and complete. It remains to solve these problems in turn. We begin in region IV. The solution to equations (96*a*, *b*) which satisfies conditions (96*c*–*g*) is readily obtained as

$$\alpha_{\rm IV}(x,\hat{t}) = \hat{t}^{\frac{1}{2}\mu_1-1}\gamma_0(x), \quad \beta_{\rm IV}(x,\hat{t}) = \beta_\infty(x), \qquad (101)$$

where $\gamma_0(x)$ and $\beta_\infty(x)$ are as defined in §3. Thus, in this region, β remains steady, with α continuing to decay algebraically for $\hat{t} = O(1)$. We proceed to region VI(*b*), where the solution to equations (100*a*, *b*) subject to conditions (100*c*–*h*) is given by

$$\hat{\alpha}_{\rm VI}(\hat{x},\hat{t}) = \mathrm{erf}\,(\hat{x}/2\hat{t}^{\frac{1}{2}}), \quad \hat{\psi}_0(\hat{x},\hat{t}) = \hat{x}^2/4\hat{t}. \qquad (102)$$

In this region, α continues to diffuse in the presence of an exponentially small diffusing layer in β. The solution (102) enables the far-field conditions (99*a*, *b*) in region VI(*a*) to be specified more precisely as $\tilde{\alpha}_{\rm VI}(x,\hat{t}) \sim x/(\pi\hat{t})^{\frac{1}{2}}, \hat{\psi}_0(x,\hat{t}) \sim x^2/4\hat{t}$ as

$x \to \infty$, $\hat{t} > 0$, after which the solution to equations (98*a*, *b*) together with conditions (98*c*–*f*) is determined as

$$\tilde{\alpha}_{\mathrm{VI}}(x, \hat{t}) = (x-\lambda)/(\pi\hat{t})^{\frac{1}{2}}, \quad \hat{\psi}_0(x, \hat{t}) = (x-\lambda)^2/4\hat{t}. \tag{103}$$

Within this region, the exponential order of β is smaller (of $O(\mathrm{e}^{-D^{-\frac{1}{2}}})$) than in region VI(*b*) (of $O(\mathrm{e}^{-D^{-1}})$). This enables the transition between the reaction and diffusion of β in region V and the weak diffusion layer of β in region VI(*b*).

It remains to consider region V. A solution to the full initial/boundary value problem (97*a*–*h*) has not been found. However, the structure of the boundary conditions (97*g*, *h*) indicates that the thickness of region V increases with $\hat{t}$, being of $O(D^{\frac{1}{4}}\hat{t}^{\frac{1}{2}})$.

We have thus far continued the solution of the full initial-value problem (7), (8) into times $t = O(D^{-\frac{1}{2}})$, and obtained a uniform representation for all $x \geqslant 0$, the structure of which contains four asymptotic regions as $D \to 0$. Region IV is the domain where the reaction has almost gone to completion, while regions VI(*a*, *b*) are dominated by diffusion in α, with a weak, exponentially small layer of β diffusing forward. Region V has a balance between reaction and diffusion of both α and β, and accommodates the development of the spike in β which formed in region II when $t = O(1)$. Although we have not obtained an explicit solution in region V, the form of equations (97*a*, *b*) suggests that the growth of the spike will be curbed in region V, and the combined effects of reaction and diffusion will lead to the initial stages of the formation of a travelling wave front. The details of this asymptotic structure when $t = O(D^{-\frac{1}{2}})$ are in good agreement with the second induction phase identified from the numerical solutions of the full initial-value problem in §2. In particular, the numerical solution illustrated in figure 1*c* shows the spreading of the spike in β during the second induction phase. This is in good agreement with the predicted thickening of region V, with thickness of $O(D^{\frac{1}{4}}\hat{t}^{\frac{1}{2}})$, that is $O(D^{\frac{1}{2}}t^{\frac{1}{2}})$.

We must now consider whether the structure we have just obtained for $\hat{t} = O(1)$ remains uniform as $\hat{t} \to \infty$. We expect this will not be the case, as the numerical solutions of §2 have shown that the final stage of the development of the solution of the full initial-value problem (7), (8) involves the propagation of a travelling wave front away from the neighbourhood of $x = \lambda$. This wave propagates with the minimum speed available for permanent form travelling waves, $v = 2\sqrt{D}$ (see BN). The presence of a further non-uniformity as $\hat{t} \to \infty$ is also indicated by the thickening of region V. When the thickness of region V becomes of $O(1)$, matching between V and VI(*a*) fails, and a non-uniformity occurs on this time scale. The thickness of region V is of $O(D^{\frac{1}{4}}\hat{t}^{\frac{1}{2}})$ and the non-uniformity thus occurs when $\hat{t} = O(D^{-\frac{1}{2}})$ which is equivalent to $t = O(D^{-1})$. It is of interest to note that this is the timescale identified in §2, from the numerical solutions, as the end of the second induction phase, when the leading edge of the travelling wave front separates from the head of the thickening spike in β. In terms of the present asymptotic analysis, this corresponds to the wave front emerging out of the coalescence of regions V and VI(*a*) when $\hat{t} = O(D^{-\frac{1}{2}})$.

To continue the asymptotic development as $D \to 0$ of the solution of the full initial-value problem (7), (8) into times $\hat{t} = O(D^{-\frac{1}{2}})[t = O(D^{-1})]$ and beyond, an examination of the behaviour of the solutions in regions IV, V, VI(*a*, *b*) reveals that three further regions must be introduced when $\tilde{t} = D^{\frac{1}{2}}\hat{t} = O(1)$. The structure of the three regions is as follows.

PHILOSOPHICAL TRANSACTIONS OF THE ROYAL SOCIETY A MATHEMATICAL, PHYSICAL & ENGINEERING SCIENCES

Region VII; $x = O(1)$, $\tilde{t} = O(1)$

$$\alpha = D^{1-\frac{1}{2}\mu_1}\,\mathrm{e}^{-(A_0 v)^{\frac{1}{2}}\tilde{t}/D^{\frac{1}{2}}}\alpha_{\mathrm{VII}}(x,\tilde{t}), \quad \beta = \beta_{\mathrm{VII}}(x,\tilde{t}) + o(1), \quad \text{as} \quad D \to 0,$$

where

$$\left.\begin{aligned} \partial^2\alpha_{\mathrm{VII}}/\partial x^2 - \alpha_{\mathrm{VII}}\beta_{\mathrm{VII}} &= 0, \\ \partial\beta_{\mathrm{VII}}/\partial\tilde{t} &= \partial^2\beta_{\mathrm{VII}}/\partial x^2, \end{aligned}\right\} \quad 0 \leqslant x < vD^{-\frac{1}{2}}\tilde{t} + \lambda, \quad \tilde{t} \geqslant 0, \tag{104a, b}$$

subject to the conditions (8*b*)

$$\partial\alpha_{\mathrm{VII}}/\partial x = \partial\beta_{\mathrm{VII}}/\partial x = 0 \quad \text{at} \quad x = 0, \quad \tilde{t} > 0, \tag{104c}$$

together with matching to IV, V as $\tilde{t} \to 0$ and to VIII as $x \to \infty$. (In the above, A_0 is a function of $\tilde{t}$ and v is a positive constant, which are determined at a later stage.)

Region VIII; $z = x - \lambda - vD^{-\frac{1}{2}}\tilde{t} = O(1)$, $\tilde{t} = O(1)$

$$\alpha = D^{\frac{1}{2}}\alpha_{\mathrm{VIII}}(z,\tilde{t}) + o(D^{\frac{1}{2}}), \quad \beta = \beta_{\mathrm{VIII}}(z,\tilde{t}) + o(1), \quad \text{as} \quad D \to 0,$$

where

$$\left.\begin{aligned} \partial^2\alpha_{\mathrm{VIII}}/\partial z^2 - \alpha_{\mathrm{VIII}}\beta_{\mathrm{VIII}} &= 0, \\ v\,\partial\beta_{\mathrm{VIII}}/\partial z + \alpha_{\mathrm{VIII}}\beta_{\mathrm{VIII}} &= 0, \end{aligned}\right\} \quad -\infty < z < \infty, \quad \tilde{t} > 0, \tag{105a, b}$$

subject to matching to V, VI(*a*) as $\tilde{t} \to 0$, VII as $z \to -\infty$ and IX as $z \to +\infty$.

Region IX; $\tilde{z} = D^{\frac{1}{2}}z = O(1)$, $\tilde{t} = O(1)$

$$\alpha = \alpha_{\mathrm{IX}}(\tilde{z},\tilde{t}) + o(1), \; \beta = D^{p+\frac{1}{2}}\exp\{-\chi_0(\tilde{z},\tilde{t})/D + o(D^{-1})\}, \quad \text{as} \quad D \to 0,$$

where

$$\left.\begin{aligned} \partial\alpha_{\mathrm{IX}}/\partial\tilde{t} &= \partial^2\alpha_{\mathrm{IX}}/\partial\tilde{z}^2 + v\,\partial\alpha_{\mathrm{IX}}/\partial\tilde{z}, \\ \partial\chi_0/\partial\tilde{t} &= v\,\partial\chi_0/\partial\tilde{z} - (\partial\chi_0/\partial\tilde{z})^2 - \alpha_{\mathrm{IX}}, \end{aligned}\right\} \quad \tilde{z} > 0, \quad \tilde{t} > 0, \tag{106a, b}$$

$$\alpha_{\mathrm{IX}}(\tilde{z},\tilde{t}) \to 1, \quad \chi_0(\tilde{z},\tilde{t}) \to \infty \quad \text{as} \quad \tilde{z} \to \infty, \quad \tilde{t} > 0, \tag{106c, d}$$

together with matching to regions VI(*a*, *b*) as $\tilde{t} \to 0$ and region VIII as $\tilde{z} \to 0$.

In each of the above regions, the forms of the expansions for α, β are indicated by the respective matching requirements to regions IV, V, VI(*a*, *b*) as $\tilde{t} \to 0$. The region VIII is in a moving frame of reference with constant displacement speed $v\sqrt{D}$ (in terms of the original coordinates x, t), where v is, at this stage, an undetermined constant of $O(1)$. This region emerges from regions V, VI(*a*) as $\tilde{t} \to 0$. Ahead of region VIII is region IX which is a weakly diffusing region where β is exponentially small and α returns to unity. This region emerges from VI(*b*) as $\tilde{t} \to 0$. Finally, behind region VIII, we have region VII which is a predominantly diffusive region that emerges from IV as $\tilde{t} \to 0$. The matching between regions IX, VIII, VII is interactive and has to be performed as we solve the problems in turn.

We begin in region VIII. On addition of equations (105*a*, *b*), we may integrate once to obtain

$$\partial\alpha_{\mathrm{VIII}}/\partial z + v\beta_{\mathrm{VIII}} = A_0(\tilde{t}), \tag{107}$$

for some undetermined function $A_0(\tilde{t})$. Equations (105*b*) and (107) are now a second-order nonlinear system, which is autonomous in z. These equations are, in fact, the equations studied in BN (see equations (21) in BN) for the permanent form unit

travelling waves of equations (7) as $D \to 0$. To match with region VII, we require $\alpha_{\mathrm{VIII}} \to 0$ as $z \to -\infty$, which, from (107), then requires $\beta_{\mathrm{VIII}} \to A_0(\tilde{t})/v$ as $z \to -\infty$. An examination of the $(\alpha_{\mathrm{VIII}}, \beta_{\mathrm{VIII}})$ phase portrait of equations (105*b*), (107) (see BN, §2) then shows that we require the unique solution of these equations, which connects the equilibrium point at $(0, A_0(\tilde{t})/v)$ to the end of the positive α_{VIII} axis. This solution has $\alpha_{\mathrm{VIII}}(z, \tilde{t})$ monotone increasing in z, while $\beta_{\mathrm{VIII}}(z, \tilde{t})$ is monotone decreasing in z. As $z \to \infty$ we have

$$\alpha_{\mathrm{VIII}}(z, \tilde{t}) \sim A_0(\tilde{t})\, z, \quad \beta_{\mathrm{VIII}}(z, \tilde{t}) \sim \mathrm{e}^{-A_0(\tilde{t}) z^2/2v}. \tag{108a, b}$$

This completes the solution in VIII, which is uniquely determined up to the function $A_0(\tilde{t})$ and the constant v. It must be shown that this solution will match with region V and VI(*a*) as $\tilde{t} \to 0$; however, this cannot be done until the function $A_0(\tilde{t})$ has been determined.

We next proceed to region IX, and begin by solving equation (106*a*) for $\alpha_{\mathrm{IX}}(\tilde{z}, \tilde{t})$. We first complete the matching conditions, which give

$$\alpha_{\mathrm{IX}}(\tilde{z}, \tilde{t}) \to 0 \quad \text{as} \quad \tilde{z} \to 0, \quad \tilde{t} > 0, \tag{109a}$$

on matching to VIII, and

$$\alpha_{\mathrm{IX}}(\tilde{z}, \tilde{t}) \sim \operatorname{erf}((\tilde{z} + v\tilde{t})/2\tilde{t}^{\frac{1}{2}}) \quad \text{as} \quad \tilde{t} \to 0, \quad \tilde{z} > 0, \tag{109b}$$

on matching to VI(*b*). The solution of equation (106*a*) subject to (106*c*), (109*a*, *b*) is readily obtained (via Laplace transforms) as

$$\alpha_{\mathrm{IX}}(\tilde{z}, \tilde{t}) = 1 - \frac{\mathrm{e}^{-\frac{1}{2}v\tilde{z}}}{2\pi\mathrm{i}} \int_{p_0 - \mathrm{i}\infty}^{p_0 + \mathrm{i}\infty} \frac{1}{p} \exp\left[-(p + \tfrac{1}{4}v^2)^{\frac{1}{2}}\tilde{z}\right] \mathrm{e}^{p\tilde{t}}\, \mathrm{d}p, \quad \tilde{z} > 0, \quad \tilde{t} > 0, \tag{110}$$

where $p_0 > 0$, the branch-cut for the square root is taken along the section $(-\infty, -\frac{1}{4}v^2)$ of the real p-axis, and $\arg(p + \frac{1}{4}v^2) = 0$ on the positive real p-axis. Although (110) can readily be rewritten as a branch-cut integral, we do not pursue this here, as all the information we require can easily be extracted from its present form. On using the initial and final value theorems (see, for example, Watson 1981), we obtain from (110), after some manipulation

$$\alpha_{\mathrm{IX}}(\tilde{z}, \tilde{t}) \sim 1 - (2\tilde{t}^{\frac{1}{2}}/\sqrt{\pi}\tilde{z}) \exp\left[-(\tilde{z} + v\tilde{t})^2/4\tilde{t}\right] \quad \text{as} \quad \tilde{t} \to 0, \quad \tilde{z} = O(1) \tag{111a}$$

$$\alpha_{\mathrm{IX}}(\tilde{z}, \tilde{t}) \sim \begin{cases} (1 - \mathrm{e}^{-v\tilde{z}}) + O(\mathrm{e}^{-\frac{1}{4}v^2\tilde{t}}), & \tilde{z} = O(1), \\ 1 - (2\tilde{t}^{\frac{1}{2}}/\sqrt{\pi}\tilde{z}) \exp\left[-(\tilde{z} + v\tilde{t})^2/4\tilde{t}\right], & \tilde{z} \gg \tilde{t}^{\frac{1}{2}}, \end{cases} \quad \text{as} \quad \tilde{t} \to \infty \tag{111b}$$

$$\alpha_{\mathrm{IX}}(\tilde{z}, \tilde{t}) \sim \left[v - \tfrac{1}{2}v\{1 - \operatorname{erf}(\tfrac{1}{2}v\tilde{t}^{\frac{1}{2}})\} + \mathrm{e}^{-\frac{1}{4}v^2\tilde{t}^2}/(\pi\tilde{t})^{\frac{1}{2}}\right]\tilde{z} \quad \text{as} \quad \tilde{z} \to 0 \quad \forall\, \tilde{t} > 0. \tag{111c}$$

The form (111*a*) agrees with the matching condition (109*b*) as $\tilde{t} \to 0$ with $\tilde{z} = O(1)$, as required. The long-time development of α_{IX}, given by (111*b*), shows a double structure. With $\tilde{z} = O(1)$ the quasi-steady travelling wave profile is developing through interaction with region VIII as $\tilde{z} \to 0$. However, the final decay to unity as $\tilde{z} \to \infty$ is through a diffusive type structure which is 'pushed' ahead of the wave front, and has emerged into region IX from region VI(*b*) as $\tilde{t} \to 0$. Finally the asymptotic form for α_{IX} as $\tilde{z} \to 0$ for all $\tilde{t} > 0$ is given in (111*c*). A further matching of α between regions VIII and IX, now up to $O(D^{\frac{1}{2}})$, gives, via (108*a*) and (111*c*)

$$A_0(\tilde{t}) = v - \tfrac{1}{2}v\{1 - \operatorname{erf}(\tfrac{1}{2}v\tilde{t}^{\frac{1}{2}})\} + \mathrm{e}^{-\frac{1}{4}v^2\tilde{t}}/(\pi\tilde{t})^{\frac{1}{2}}. \tag{112}$$

We now turn to equation (106*b*) for $\chi_0(\tilde{z},\tilde{t})$. The matching conditions required to complete the initial/boundary value problem for $\chi_0(\tilde{z},\tilde{t})$ are obtained as

$$\chi_0(\tilde{z},\tilde{t}) \sim (\tilde{z}+v\tilde{t})^2/4\tilde{t} \quad \text{as} \quad \tilde{t}\to 0, \quad \tilde{z}>0, \tag{113a}$$

on matching to VI(*b*), and

$$\chi_0(\tilde{z},\tilde{t}) \sim A_0(\tilde{t})\tilde{z}^2/2v \quad \text{as} \quad \tilde{z}\to 0, \quad \tilde{t}>0, \tag{113b}$$

on matching to VIII. In addition we have condition (106*d*) as $\tilde{z}\to\infty$, $\tilde{t}>0$. The boundary-value problem posed by (106*b*, *d*), (113*a*, *b*) is nonlinear and inhomogeneous, and we have been unable to obtain an exact solution. However, we are able to obtain the solution for large and small $\tilde{t}$. This is sufficient to show that this boundary-value problem is an eigenvalue problem for v, and has a single eigenvalue which we determine. We first obtain the leading order asymptotic form of the solution of the boundary-value problem when $\tilde{z}\gg\tilde{t}^{\frac{1}{2}}$, which includes the asymptotic form as $\tilde{t}\to 0$ for all $\tilde{z}>0$ together with the asymptotic form as $\tilde{t}\to\infty$ for $\tilde{z}\gg\tilde{t}^{\frac{1}{2}}$. The form of the initial condition (113*a*) suggests that we should look for a solution of the form

$$\chi_0(\tilde{z},\tilde{t}) \sim \tilde{t}F(\tilde{z}/\tilde{t}), \quad \tilde{z}\gg\tilde{t}^{\frac{1}{2}}. \tag{114}$$

On substitution into equation (106*b*) we arrive at the exact equation

$$[F'(\hat{z})]^2-(v+\hat{z})F'(\hat{z})+F(\hat{z})+\alpha_{\mathrm{IX}}(\tilde{z},\tilde{t})=0, \tag{115}$$

where $\hat{z}=\tilde{z}/\tilde{t}$. Now, for $\tilde{z}\gg\tilde{t}^{\frac{1}{2}}$, α_{IX} may be approximated via (111*b*), so that $\alpha_{\mathrm{IX}}=1+O((\tilde{t}^{\frac{1}{2}}/\tilde{z})\,\mathrm{e}^{-\tilde{z}^2/4\tilde{t}})$ for $\tilde{z}\gg\tilde{t}^{\frac{1}{2}}$. Thus, (115) becomes

$$[F'(\hat{z})]^2-(v+\hat{z})F'(\hat{z})+F(\hat{z})+1=0 \tag{116}$$

at leading order when $\tilde{z}\gg\tilde{t}^{\frac{1}{2}}$ (in fact up to terms exponentially small in $\tilde{z}\tilde{t}^{-\frac{1}{2}}$). It is readily shown that equation (116) has the one parameter family of linear solutions

$$F(\hat{z};c)=c\hat{z}+cv-c^2-1 \tag{117a}$$

for any $c\in\mathbb{R}$. Also, the envelope of the family of curves (117*a*) provides a solution of (116) as

$$F_{\mathrm{e}}(\hat{z})=\tfrac{1}{4}(\hat{z}+v)^2-1. \tag{117b}$$

Local existence and uniqueness results for first-order ordinary differential equations (see, for example, Coddington & Levinson 1955), then demonstrate that (117*a*, *b*) provide the general solution to (116). The initial condition (113*a*) requires that we choose the envelope solution (117*b*) of (116). Thus we have, via (117*b*), (114)

$$\chi_0(\tilde{z},\tilde{t}) \sim \tilde{t}[\tfrac{1}{4}(\hat{z}+v)^2-1], \quad \tilde{z}\gg\tilde{t}^{\frac{1}{2}}. \tag{118}$$

Now, the asymptotic form for $\chi_0(\tilde{z},\tilde{t})$ as $\tilde{t}\to\infty$ is given by (118) when $\tilde{z}\gg\tilde{t}^{\frac{1}{2}}\gg 1$, that is for large $\tilde{z}$. However, for $\tilde{t}\gg 1$, the boundary condition (113*b*), to be satisfied by $\chi_0(\tilde{z},\tilde{t})$ as $\tilde{z}\to 0$, becomes

$$\chi_0(\tilde{z},\tilde{t}) \sim \tfrac{1}{2}\tilde{z}^2 \quad \text{as} \quad \tilde{z}\to 0, \quad \tilde{t}\gg 1, \tag{119}$$

via (112). This condition cannot be satisfied by (118) as $\tilde{z}\to 0$, and we conclude that the approximation (118) fails when $\tilde{z}=O(1)$ as $\tilde{t}\to\infty$. The form of condition (119) suggests that

$$\chi_0(\tilde{z},\tilde{t}) \sim \chi_s(\tilde{z})+o(1), \quad \tilde{z}=O(1) \quad \text{as} \quad \tilde{t}\to\infty. \tag{120a}$$

PHILOSOPHICAL TRANSACTIONS OF THE ROYAL SOCIETY A MATHEMATICAL, PHYSICAL & ENGINEERING SCIENCES

On substitution into equation (106*b*) we obtain, after use of (111*b*)

$$[\chi_s'(\tilde{z})]^2 - v\chi_s'(\tilde{z}) + (1 - \mathrm{e}^{-v\tilde{z}}) = 0. \tag{120b}$$

The solution of (120*b*) which satisfies the condition (119) is readily obtained as

$$\chi_s(\tilde{z}) = \frac{1}{2}\int_0^{\tilde{z}} [v - (v^2 - 4(1 - \mathrm{e}^{-vs}))^{\frac{1}{2}}]\,\mathrm{d}s; \quad \tilde{z} > 0. \tag{120c}$$

The approximations (118), (120*a*, *c*) thus provide a uniform approximation to χ_0 as $\tilde{t} \to \infty$ for all $\tilde{z} \geqslant 0$. It remains to match (120*a*) as $\tilde{z} \to \infty$, with (118) as $\hat{z} \to 0$. The expansion to $O(1)$ when $\tilde{z} = O(1)$, given by (120*a*, *c*), expanded when $\hat{z} = O(1)$ to $O(\tilde{t})$, leads to

$$\chi_0^{(1,\tilde{t})} = \tfrac{1}{2}[v - (v^2 - 4)^{\frac{1}{2}}]\tilde{z}. \tag{121a}$$

However, the expansion to $O(\tilde{t})$ when $\hat{z} = O(1)$, given by (118), expanded when $\tilde{z} = O(1)$ to $O(1)$, results in

$$\chi_0^{(\tilde{t},1)} = \tilde{t}[\tfrac{1}{4}v^2 - 1] + \tfrac{1}{2}v\tilde{z}. \tag{121b}$$

The matching principle (see, for example, Van Dyke 1975) requires $\chi_0^{(\tilde{t},1)} \equiv \chi_0^{(1,\tilde{t})}$ for all $\tilde{z} > 0$ as $\tilde{t} \to \infty$. A comparison of (121*a*, *b*) then requires

$$v = 2, \tag{122}$$

after which the solutions match at leading order. This completes the details of the solution in region IX. The problem for α_{IX}, on matching to region VIII, determined the function $A_0(\tilde{t})$, whilst the problem for χ_0 was an eigenvalue problem for v, with the single eigenvalue $v = 2$. This then gives the propagation speed of the developing travelling wave in regions VIII, IX, as $2\sqrt{D}$ (in terms of the original coordinates x, t). Thus, in the long time, the present initial-value problem (7), (8), develops a travelling wave with minimum propagation speed (there is a family of travelling waves with speed $v_0 \geqslant 2\sqrt{D}$ for each $D > 0$, see BN). It is interesting to note that this minimum speed requirement is determined in the region ahead of the main travelling wave, where β is exponentially small, with a balance in weak diffusion and reaction ahead of the main wave limiting its propagation speed. This is in excellent agreement with the numerical solutions of §2.

With $A_0(\tilde{t})$ and v now determined, we return to region VIII. Since $A_0(\tilde{t}) \to v$ as $\tilde{t} \to \infty$, we see, via (105*b*), (107), (108*a*, *b*), (112*b*), that $\alpha_{\mathrm{VIII}}(z, \tilde{t})$ and $\beta_{\mathrm{VIII}}(z, \tilde{t})$ approach the permanent form wave profile for the minimum speed unit travelling wave as $D \to 0$ (see BN, §2). To the rear of the wave, as $z \to -\infty$, we have

$$\beta_{\mathrm{VIII}}(z, \tilde{t}) \to \tfrac{1}{2}A_0(\tilde{t}) \sim \begin{cases} 1 + (1/8\pi^{\frac{1}{2}}\tilde{t}^{\frac{3}{2}})\,\mathrm{e}^{-\tilde{t}}, & \tilde{t} \to \infty \\ 1/2(\pi\tilde{t})^{\frac{1}{2}}, & \tilde{t} \to 0 \end{cases} \tag{123}$$

Thus, at the rear of the developing travelling wave, the concentration β decreases from its initial level on leaving the diffusing spike as $\hat{t} \to \infty$ in region V, and approaches its permanent form value of unity for a unit travelling wave, as $\tilde{t} \to \infty$ in region VIII. This completes all the details in regions VIII and IX. It remains only to consider region VII at the rear of the developing travelling wave.

In region VII we consider first the problem for $\beta_{\mathrm{VII}}(x, \tilde{t})$. This consists of the

diffusion equation (104*b*) together with condition (104*c*) and the following matching conditions

$$\beta_{\mathrm{VII}}(x,\tilde{t}) \to \frac{1}{v} A_0(\tilde{t}) \quad \text{as} \quad x \to vD^{-\frac{1}{2}}\tilde{t} + \lambda, \quad \tilde{t} > 0, \tag{124a}$$

$$\beta_{\mathrm{VII}}(x,\tilde{t}) \to \beta_\infty(x) \quad \text{as} \quad \tilde{t} \to 0, \quad 0 \leqslant x < \lambda. \tag{124b}$$

The full problem (104*b*) subject to (104*c*) and (124*a*, *b*) constitutes a moving boundary problem for the diffusion equation. As this region is passive and the important wave front structures have already been considered, we do not pursue this problem in detail. However, conditions (124*a*) and (104*c*), together with (112*b*) and (122), show that

$$\beta_{\mathrm{VII}}(x,\tilde{t}) \sim 1 + O(\tilde{t}^{-\frac{1}{2}}), \quad 0 \leqslant x < vD^{-\frac{1}{2}}\tilde{t} + \lambda, \tag{124c}$$

as $\tilde{t} \to \infty$. The problem for $\alpha_{\mathrm{VII}}(x,\tilde{t})$ is given by (104*a*), (104*c*) and the matching conditions

$$\alpha_{\mathrm{VII}}(x,\tilde{t}) \sim \tilde{t}^{\frac{1}{2}\mu_1 - 1}\gamma_0(x) \quad \text{as} \quad \tilde{t} \to 0, \quad 0 \leqslant x < vD^{-\frac{1}{2}}\tilde{t} + \lambda, \tag{125a}$$

$$\alpha_{\mathrm{VII}}(x,\tilde{t}) = O(\mathrm{e}^{(A_0/v)^{\frac{1}{2}}x}) \quad \text{for} \quad x \sim vD^{-\frac{1}{2}}\tilde{t} + O(1), \quad t > 0. \tag{125b}$$

Again, we show, via (104*a*), (104*c*), (124*c*), (112*b*) and (122), that

$$\alpha_{\mathrm{VII}}(x,\tilde{t}) \sim C_\infty \cosh x \quad \text{as} \quad \tilde{t} \to \infty, \tag{125c}$$

for some fixed constant C_∞. Thus, in region VII as $\tilde{t} \to \infty$, β diffuses down to the level of unity which is fixed behind the wave front, through terms of $O(\tilde{t}^{-\frac{1}{2}})$, whilst α_{VII} has a cosh profile, which decays to zero exponentially in $\tilde{t}$. The early time behaviour in region VII encompasses the passive diffusion of the spike in β, left behind after the departure of the travelling wave in region VIII.

The structure when $t = O(D^{-1})$ is now complete. An examination of the leading order solutions in each of regions VII, VIII and IX as $\tilde{t} \to \infty$, shows that this structure remains uniform as $\tilde{t} \to \infty$, for all $x > 0$. The asymptotic solution of the full initial value problem (7), (8) is thus complete. We have seen that the evolution of α, β takes place on three distinct time scales, $t = O(1)$, $O(D^{-\frac{1}{2}})$, $O(D^{-1})$. These correspond well to the timescales associated with the induction phases observed in the numerical solutions of (7), (8) in §2. The spatial structure on each timescale is also in excellent agreement with the numerical solutions. On the final timescale $t = O(D^{-1})$, a permanent form unit travelling wave develops and propagates out with the minimum available speed, $2\sqrt{D}$, which was determined by a nonlinear eigenvalue problem in region IX, for the leading order exponentially small term in β. A schematic diagram illustrating the asymptotic structure of the solution to the full initial value problem (7), (8) is shown on the (t, x) plane in figure 16.

By constructing a formal asymptotic solution to (7), (8) as $D \to 0$, uniform for all $x, t \geqslant 0$, we have established the following theorem.

Theorem 4.1. *With* $0 < D \ll 1$, *the solution of the initial-value problem* (7), (8), $\alpha(x,t)$, $\beta(x,t)$, *up to leading order in matched asymptotic expansions, converges to the permanent form unit travelling wave solution of equations* (7) *with minimum propagation speed* $2\sqrt{D}$ (*see BN* §2), *in the sense that*

$$\left.\begin{matrix}\alpha(y+ct,t)\\ \beta(y+ct,t)\end{matrix}\right\} \to \begin{cases}\left.\begin{matrix}1\\0\end{matrix}\right\}, & c > 2\sqrt{D},\\ \left.\begin{matrix}0\\1\end{matrix}\right\}, & 0 \leqslant c < 2\sqrt{D},\end{cases}$$

PHILOSOPHICAL TRANSACTIONS OF THE ROYAL SOCIETY A MATHEMATICAL, PHYSICAL & ENGINEERING SCIENCES

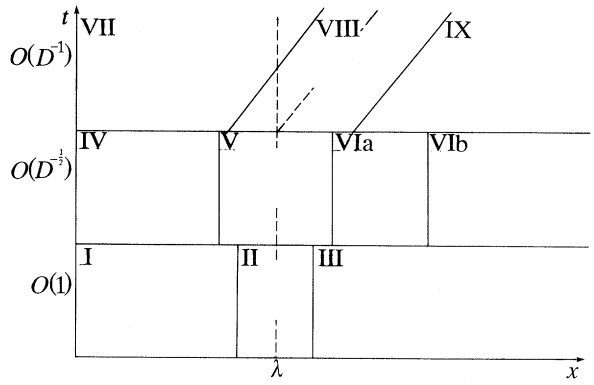

Figure 16. A sketch of the ten asymptotic regions of the solution of the initial value problem (7), (8) with $n = 1$, as $D \to 0$. I, $\alpha = O(1)$, $\beta = O(1)$, $0 \leqslant x < \lambda - O(D^{\frac{1}{2}})$; II, $\alpha = O(1)$, $\beta = O(D^{\frac{1}{2}p})$, $|\lambda - x| = O(D^{\frac{1}{2}})$; III, $\alpha = O(1)$, $\beta = D^{p+\frac{1}{2}} e^{-D^{-1}\psi}$, $\psi = O(1)$, $x > \lambda + O(D^{\frac{1}{2}})$; IV, $\alpha = O(D^{\frac{1}{2}-\frac{1}{4}\mu})$, $\beta = O(1)$, $0 \leqslant x < \lambda - O(D^{\frac{1}{4}})$; V, $\alpha = O(D^{\frac{1}{4}})$, $\beta = O(D^{-\frac{1}{2}})$, $|\lambda - x| = O(D^{\frac{1}{4}})$; VI(*a*), $\alpha = O(D^{\frac{1}{4}})$, $\beta = D^{p+\frac{1}{2}} e^{-D^{-\frac{1}{2}}\tilde{\psi}} \tilde{\psi} = O(1)$, $x = \lambda + O(1)$; VI(*b*), $\alpha = O(1)$, $\beta = D^{p+\frac{1}{2}} e^{-D^{-1}\hat{\psi}}$, $\hat{\psi} = O(1)$, $x = \lambda + O(D^{\frac{1}{4}})$; VII, $\alpha = D^{1-\frac{1}{2}\mu_1} e^{-D^{-\frac{1}{2}}\rho}$, $\rho = O(1)$, $\beta = O(1)$, $x = O(1)$; VIII, $\alpha = O(D^{\frac{1}{2}})$, $\beta = O(1)$, $x = \lambda + vD^{\frac{1}{2}}t + O(1)$; IX, $\alpha = O(1)$, $\beta = D^{p+\frac{1}{2}} e^{-D^{-1}\chi}$, $\chi = O(1)$, $x = \lambda + vD^{\frac{1}{2}}t + O(D^{-\frac{1}{2}})$.

as $t \to \infty$ *for all* $y > 0$. *In addition, the convergence is approached over a timescale* $t = O(D^{-1})$ *as* $D \to 0$.

The initial-value problem (7), (8) has initial conditions with compact support in β. This is crucial in obtaining the asymptotic structure of the solution of the initial value problem as $D \to 0$. The structure for initial conditions without compact support would have to be modified and may lead to the generation of faster permanent form unit travelling waves. Results of the type given by Theorem 4.1 have been proved rigorously for scalar reaction–diffusion equations of the Fisher type by McKean (1975), Fife & McLeod (1977) and Larson (1978) who showed, in particular, that initial conditions with compact support lead to minimum speed travelling waves.

Theorem 4.1 formally extends these results to the coupled system of reaction–diffusion equations (7).

(*b*) *Cubic autocatalysis,* $n = 2$

$p = 0$, $g(x)$ is discontinuous at $x = \lambda$

When $p = 0$, equations (84*b*) and (86) give

$$\partial \beta_{\mathrm{II}} / \partial t = \partial^2 \beta_{\mathrm{II}} / \partial X^2 + A(t) \beta_{\mathrm{II}}^2, \quad -\infty < X < \infty, \quad t > 0, \tag{126a}$$

which is to be solved subject to the initial condition (87*b*), and the matching conditions

$$\beta_{\mathrm{II}}(X, t) \sim \beta_0 g_\lambda \left\{ 1 - \beta_0 g_\lambda \int_0^t A(\tau)\, \mathrm{d}\tau \right\}^{-1}, \quad X \to -\infty, \quad t \geqslant 0, \tag{126b}$$

$$\beta_{\mathrm{II}}(X, t) \to 0, \quad X \to +\infty, \quad t \geqslant 0, \tag{126c}$$

via (10*b*), where $A(t)$ is as defined in (86). In particular, for $n = 2$, we have

$$A(t) \sim A_\infty t^{-\frac{1}{2}} e^{-2\sigma t^{\frac{1}{2}}}, \quad t \to \infty, \tag{126d}$$

on using (61). In the absence of the complete details of $A(t)$, we are unable to solve the initial/boundary value problem (126*a–c*) exactly. However, the small time solution is readily obtained as (using $A(t) \sim 1$ as $t \to 0$)

$$\beta_{\mathrm{II}}(X,t) \sim \tfrac{1}{2}\beta_0 g_\lambda[1-\mathrm{erf}\{X/2t^{\frac{1}{2}}\}] \quad \text{as} \quad t \to 0, \quad -\infty < X < \infty. \tag{127}$$

This behaviour is again due to diffusive smoothing of the initial discontinuity in β, with a thin, exponentially small (as $t \to 0$) layer of β diffusing into $x > \lambda$. We next consider the long time behaviour of the solution of the problem (126*a–c*). Although we have been unable to find the precise long time asymptotic development of the solution we have obtained upper and lower solutions which bound $\beta_{\mathrm{II}}(X,t)$ for all $|X|$, $t \geqslant 0$, and provide interesting information about the behaviour of $\beta_{\mathrm{II}}(X,t)$ as $t \to \infty$. In the Appendix we show that

$$\beta(X,t) \leqslant \beta_{\mathrm{II}}(X,t) \leqslant \bar{\beta}(X,t), \quad |X|, t \geqslant 0, \tag{128a}$$

where

$$\bar{\beta}(X,t) = \tfrac{1}{2}F(t)\ \mathrm{erfc}\ (X/2t^{\frac{1}{2}}), \tag{128b}$$

$$\beta(X,t) = \tfrac{1}{2}F(t)\ \mathrm{erfc}\left(\frac{X}{2t^{\frac{1}{2}}}\right)\left[1-\beta_0 g_\lambda \int_0^t A(\tau)\,\mathrm{d}\tau\right] \Big/ \left[1-\tfrac{1}{2}\beta_0 g_\lambda\ \mathrm{erfc}\left(\frac{X}{2t^{\frac{1}{2}}}\right)\int_0^t A(\tau)\,\mathrm{d}\tau\right], \tag{128c}$$

and

$$F(t) = \beta_0 g_\lambda \Big/ \left\{1-\beta_0 g_\lambda \int_0^t A(\tau)\,\mathrm{d}\tau\right\}. \tag{128d}$$

We note that both the upper and lower solutions satisfy the initial condition (87*b*) and the boundary conditions (126*b*, *c*). Also, via equations (64), (126*d*) we obtain

$$\int_0^t A(\tau)\,\mathrm{d}\tau \sim (1/\beta_0 g_\lambda) - A_\infty\, \mathrm{e}^{-2\sigma t^{\frac{1}{2}}}/\sigma \quad \text{as} \quad t \to \infty, \tag{129a}$$

and therefore

$$F(t) \sim \sigma\, \mathrm{e}^{2\sigma t^{\frac{1}{2}}}/A_\infty \quad \text{as} \quad t \to \infty. \tag{129b}$$

Thus the upper and lower solutions remain bounded for all finite t, and hence so does $\beta_{\mathrm{II}}(X,t)$; that is, blow up in finite time cannot occur for the boundary-value problem (126*a–c*). An examination of (128*b*, *c*), (129*a*, *b*) shows that, for $|X| \gg t^{\frac{1}{2}}$

$$\bar{\beta}(X,t) - \beta(X,t) = \begin{cases} O(\mathrm{e}^{2\sigma t^{\frac{1}{2}}}\mathrm{e}^{-X^2/4t}), & X \gg t^{\frac{1}{2}}. \\ O(\mathrm{e}^{4\sigma t^{\frac{1}{2}}}\mathrm{e}^{-X^2/4t}), & (-X) \gg t^{\frac{1}{2}}, \end{cases} \tag{130a}$$

as $t \to \infty$. Thus, for $|X|$ sufficiently large, the difference between the upper and lower solutions becomes exponentially small, and we may expect that either of $\bar{\beta}(X,t)$ or $\beta(X,t)$ may provide a reasonable approximation to $\beta_{\mathrm{II}}(X,t)$. To proceed further we thus, tentatively, use $\bar{\beta}(X,t)$ to infer the structure of $\beta_{\mathrm{II}}(X,t)$ as $t \to \infty$ with $|X| \gg 1$. An examination of (128*b*) shows that

$$\bar{\beta}(X,t) \sim \begin{cases} (\sigma t^{\frac{1}{2}}/\sqrt{\pi} A_\infty X)\ \exp\,[-(X^2 - 8\sigma t^{\frac{3}{2}})/4t], & X \gg t^{\frac{1}{2}}, \\ (\sigma/A_\infty)\,\mathrm{e}^{2\sigma t^{\frac{1}{2}}}, & (-X) \gg t^{\frac{1}{2}}, \end{cases} \tag{130b}$$

as $t \to \infty$. From (130*b*) we see that two levels of structure develop as $t \to \infty$. First, the far field for $|X|$ large is not reached until $|X| \gg t^{\frac{1}{2}}$, and thus the thickness of region II increases like $O(t^{\frac{1}{2}})$. At the rear, with $(-X) \gg t^{\frac{1}{2}}$, $\bar{\beta}$ achieves the uniform, maximum value in the spike in region I, which is exponentially large as $t \to \infty$. Ahead, for $X \gg t^{\frac{1}{2}}$, $\bar{\beta}$ is exponentially small for $X \gg 2\sqrt{2}\sigma^{\frac{1}{2}}t^{\frac{3}{4}}$, but exponentially large for $t^{\frac{1}{2}} \ll X \ll 2\sqrt{2}\sigma^{\frac{1}{2}}t^{\frac{3}{4}}$. The transition occurs when

$$X \sim 2\sqrt{2}\sigma^{\frac{1}{2}}t^{\frac{3}{4}} - (\sqrt{2}/8\sigma^{\frac{1}{2}})\,t^{\frac{1}{4}} \ln t + O(t^{\frac{1}{4}}), \tag{131}$$

and $\bar{\beta}$ is of $O(1)$. Thus, within the structure developing for $X \gg t^{\frac{1}{2}}$, there is a wave front forming which, in terms of the original coordinates (x, t), is propagating with speed

$$v_\omega(t) \sim \tfrac{3}{\sqrt{2}} D^{\frac{1}{2}}\sigma^{\frac{1}{2}}t^{-\frac{1}{4}} \quad \text{as} \quad t \to \infty, \tag{132}$$

and separates the region where $\bar{\beta}$ is exponentially large in t, from that where it is exponentially small in t, as $t \to \infty$. We note that the wave speed is of $O(D^{\frac{1}{2}})$ and is decreasing in t.

The above arguments have enabled us to obtain information about the structure of the solution to the leading order boundary-value problem in region II, (126*a–c*), despite being unable to obtain a solution directly. It is interesting to note that the developing wave front at the head of region II (which is not present in the solution for region II under quadratic autocatalysis) is in accord with the numerical solutions of §2, where a decelerating wave was observed to advance away from the head of the spike in β towards the end of the second induction phase. It is now clear why this behaviour occurs for $n = 2$ (cubic) but not for $n = 1$ (quadratic). The wave structure occurs for $n = 2$ through the interaction of the product of the exponentially large reaction term and the exponentially small diffusion term for $X, t \gg 1$, in (130*b*). However, with $n = 1$, the reaction term is only algebraically large, of $O(t)$ (see (90*b*) with $A(t) \sim A_\infty t^{-1}$ as $t \to \infty$), and is always dominated by the exponentially small diffusion term at the head of region II.

At this stage we have a uniform approximation to the solution of the full initial-value problem (7), (8) for $t = O(1)$, through regions I, II and III. However, this approximation does not remain uniform as $t \to \infty$. A local non-uniformity occurs in region II, near $x = \lambda$, as $t \to \infty$. There are two possible sources for this non-uniformity.

1. The thickness of region II in $x < \lambda$ becomes comparable to the thickness of the self-similar structure containing the spike in β near $x = \lambda$, in region I. This occurs when $\mathrm{e}^{-2\sigma t^{\frac{1}{2}}} = O(D^{\frac{1}{2}}t^{\frac{1}{2}})$, via (130*b*) and (23), (30*b*), which gives the time scale for this non-uniformity as $t = O([\ln D]^2)$. The non-uniformity is then located at $0 < (\lambda - x) = O(D^{\frac{1}{2}}[-\ln D])$, with $\alpha = O(D^{\frac{1}{2}})$ and $\beta = O(D^{-\frac{1}{2}}[-\ln D]^{-1})$.

2. The advancing, decelerating wave front formed in region II, advances up to the receding diffusion front in α_{III}, which forms in region III as $t \to \infty$ (see (80*c*)). This occurs, via (131), when $D^{\frac{1}{2}}t^{\frac{3}{4}} = O(t^{\frac{1}{2}})$, which leads to the estimate $t = O(D^{-2})$ as the time scale for the development of this non-uniformity. The non-uniformity thus occurs when $x = \lambda + O(D^{-1})$ with $\beta = O(1)$ and $\alpha = O(1)$. The speed of the advancing wave front $v_\omega(t) = O(D)$ (via (132)) as the non-uniformity develops, which is the order of the minimum speed for permanent form unit travelling waves when $n = 2$ (see BN). This suggests that the minimum speed travelling wave emerges out of this non-uniformity.

To develop the asymptotic solution into times of $O([\ln D]^2)$, and up to and beyond $O(D^{-2})$, further regions must be introduced to accommodate the two non-uniformities

identified above. However, due to the lack of information concerning the precise nature of the long time solution in region II, we have been unable to deduce consistently the nature of the spatial asymptotic structure on the above, long timescales. However, the non-uniformity (1) suggests that the first induction phase, when the spike in β achieves its maximum value, ends when $t = O([\ln D]^2)$, whilst non-uniformity (2) indicates that the minimum speed travelling wave emerges from a decelerating wave when $t = O(D^{-2})$. Both of these results are in good agreement with the numerical solutions in §2, as illustrated for a particular case in figure 3*a–d*. In terms of the notation of §2, we have $t_{\mathrm{I}} = O([\ln D]^2)$, $\beta_{\max}(t_{\mathrm{I}}) = O(D^{-\frac{1}{2}}[-\ln D]^{-1})$ and $t_{\mathrm{III}} = O(D^{-2})$, which are in good agreement with numerical results given in table 2. Finally, we note that the above analysis indicates that the asymptotic structure for $X \gg t^{\frac{1}{2}}$ in region II remains uniform for $t_{\mathrm{I}} < t < t_{\mathrm{III}}$. This implies that the second induction phase $t_{\mathrm{I}} < t < t_{\mathrm{II}}$, has the same asymptotic structure as the first travelling wave propagation phase, $t_{\mathrm{II}} < t < t_{\mathrm{III}}$, and simply represents the period before the wave front has visibly emerged from the spike in β.

$p = 1, 2, \ldots$; $g(x)$ is continuous at $x = \lambda$

In this case, β_{II} satisfies equation (84*c*) in region II. The matching condition with region I is readily obtained from equation (10*b*) as

$$\beta_{\mathrm{II}} \sim \beta_0 g_\lambda (-X)^p, \quad \text{as} \quad X \to -\infty, \tag{133a}$$

whilst matching with region III leads to

$$\beta_{\mathrm{II}} \to 0 \quad \text{as} \quad X \to \infty, \tag{133b}$$

with the initial condition given by (91*b*). We now seek a similarity solution of the form

$$\beta_{\mathrm{II}}(X, t) = t^{\frac{1}{2}p} \hat{B}(\bar{\eta}), \quad \bar{\eta} = X/t^{\frac{1}{2}}. \tag{134}$$

On substituting into (84*c*), we obtain the boundary-value problem

$$\mathrm{d}^2 \hat{B}/\mathrm{d}\bar{\eta}^2 + \tfrac{1}{2}\bar{\eta}\, \mathrm{d}\hat{B}/\mathrm{d}\bar{\eta} - \tfrac{1}{2}p\hat{B} = 0, \quad |\bar{\eta}| \geqslant 0, \tag{135a}$$

$$\hat{B} \sim \beta_0 g_\lambda (-\bar{\eta})^p \quad \text{as} \quad \bar{\eta} \to -\infty, \tag{135b}$$

$$\hat{B} \to 0 \quad \text{as} \quad \eta \to \infty. \tag{135c}$$

This is identical to the boundary-value problem (92*a*, *b*) which arose in the corresponding case under quadratic autocatalysis, and therefore $\hat{B}(\bar{\eta}) \equiv \omega(\bar{\eta})$ which is given by equations (93). This solution again represents the slow diffusion of the autocatalyst, B, into the region $x > \lambda$, and shows that region II has width of $O(D^{\frac{1}{2}}t^{\frac{1}{2}})$. However, in this case, our analysis of the leading order solution in region I, given in §3*b*, shows that a spike in β forms away from the immediate neighbourhood of the point $x = \lambda$ and drifts towards this point extremely slowly. We therefore expect that the first non-uniformity arises in the solution of the initial-value problem at $t = O(D^{-1})$ when the width of region II becomes of $O(1)$. This indicates that $t_{\mathrm{I}} = O(D^{-1})$ consistent with the numerical results outlined in §2. For $t > t_{\mathrm{I}}$ the behaviour of the solution is as described above for the case $p = 0$. We also note that, for $p = 1, 2, \ldots$, we consider that the second induction phase is absent ($t = t_{\mathrm{II}}$), since the emerging wavefront is clearly visible when $t = t_{\mathrm{I}}$.

We have now analysed the initial-value problem (7), (8) for $0 < D \ll 1$ with initial input functions $g(x)$ in each of the classes $P^{(1)}$, $P^{(2)}$ and $Q^{(2)}$, defined in (81). If

$g(x) \in Q^{(1)}$ (that is if $n = 1$ and $g(x) = o((\lambda - x)\, p)$ as $x \to \lambda^-, \forall\, p \in \mathbb{N}$), then, guided by the behaviour of the solution for $g(x) \in Q^{(2)}$, we expect that the second induction phase will be absent, since the spike in β will not interact with the solution in region II. The spike will therefore continue to grow until $t = t_{\mathrm{I}} = t_{\mathrm{II}} = O(D^{-1})$, when we expect that the minimum speed travelling wave forms and propagates away from the spike. The behaviour of the solutions is summarized below.

Comparison of asymptotic solutions of the initial-value problem (7), (8) *for* $0 < D \ll 1$ *under quadratic and cubic autocatalysis*

$g(x) \in P^{(n)}$: *first induction phase*, $0 \leqslant t \leqslant t_{\mathrm{I}}$

Quadratic. A spike in β forms in the immediate neighbourhood of the point $x = \lambda$, with $\beta_{\max}(t) = O(t)$. The spike stops growing when $t = t_{\mathrm{I}} = O(D^{-\frac{1}{2}})$ and $\beta_{\max}(t_{\mathrm{I}}) = O(D^{-\frac{1}{2}})$.

Cubic. A spike in β forms in the immediate neighbourhood of the point $x = \lambda$, with $\beta_{\max}(t) = O(\mathrm{e}^{2\sigma t^{\frac{1}{2}}})$. The spike stops growing when

$$t = t_{\mathrm{I}} = O((\ln D)^2)) \quad \text{and} \quad \beta_{\max}(t_{\mathrm{I}}) = O(-D^{\frac{1}{2}}(\ln D)^{-1}).$$

As $D \to 0$, $D^{-\frac{1}{2}} \gg (\ln D)^2$, and hence the first induction phase is much longer under quadratic autocatalysis than under cubic autocatalysis, since the spike in β grows much faster in the latter case. However, for $1.8 \times 10^{-4} \lesssim D \lesssim 0.24$, $(\ln D)^2 > D^{-\frac{1}{2}}$, which includes the range of values of D that we investigated numerically in §2. In particular, for $D = 0.01$, $D^{-\frac{1}{2}} = 10$ and $(\ln D)^2 \approx 21.2$, so that t_{I} is of a similar duration under both quadratic and cubic autocatalysis.

$g(x) \in P^{(n)}$: *second induction phase*, $t_{\mathrm{I}} \leqslant t \leqslant t_{\mathrm{II}}$

Quadratic. The spike in β spreads and a wave front forms at the leading edge of the spike at $t = t_{\mathrm{II}} = O(D^{-1})$ and propagates away at the minimum speed, $v = v_1^*(D) \equiv 2\sqrt{D}$.

Cubic. The spike in β spreads and a wave front, which forms within the spike, emerges when $t = t_{\mathrm{II}}$. This wave front propagates away with speed $v \sim \frac{3}{\sqrt{2}} D^{\frac{1}{2}} \sigma^{\frac{1}{2}} t^{-\frac{1}{4}}$ for $1 \ll t \ll O(D^{-2})$, and causes the spike to spread asymmetrically.

$g(x) \in P^{(n)}$: *travelling wave propagation*, $t \geqslant t_{\mathrm{II}}$

Quadratic. The minimum speed travelling wave propagates away, whilst diffusion slowly smooths out the spike in β.

Cubic. First phase, $t_{\mathrm{II}} \leqslant t \leqslant t_{\mathrm{III}}$. The wave front decelerates as it propagates away, whilst both the concentration β and the concentration gradient β_x slowly decrease in the wave front. The propagation speed, $v \to v_2^*(D) = O(D)$ as $t \to t_{\mathrm{III}} = O(D^{-2})$, when the minimum speed travelling wave forms. This travelling wave therefore takes much longer to form under cubic autocatalysis than under quadratic autocatalysis.

Cubic. Second phase, $t \geqslant t_{\mathrm{III}}$. The minimum speed travelling wave propagates away to infinity. Diffusion has reduced the spike in β to a long hump when $t = t_{\mathrm{III}}$, and causes it to slowly decay away to unity as $t \to \infty$.

$g(x) \in Q^{(n)}$

Quadratic. A spike in β forms, but not in the immediate neighbourhood of the point $x = \lambda$. The spike stops growing when $t = t_{\mathrm{I}} = O(D^{-1})$, and a wave front forms at the leading edge of the spike. This wave front propagates away at the minimum speed, $v = v_1^*(D) \equiv 2\sqrt{D}$.

PHILOSOPHICAL TRANSACTIONS OF THE ROYAL SOCIETY A MATHEMATICAL, PHYSICAL & ENGINEERING SCIENCES

Cubic. A spike in β forms, but not in the immediate neighbourhood of the point $x = \lambda$. The spike stops growing when $t = t_{\mathrm{I}} = O(D^{-1})$ and a wave front, which forms within the spike, emerges. This wave front propagates away, causing the spike to spread asymmetrically, and the behaviour of the solution for $t \geqslant t_{\mathrm{I}} = t_{\mathrm{II}}$ is as described above for $g(x) \in P^{(2)}$.

This summary completes our analysis of the initial-value problem (7), (8) for $0 < D \ll 1$.

5. Conclusion

In this paper we have analysed the behaviour of solutions of the initial-value problem (7), (8) for $0 \leqslant D \ll 1$, which models the development of a travelling wave in a quadratic or cubic autocatalytic chemical reaction when the autocatalyst is either immobilized or diffuses slowly. Our results are summarized at the end of §3 and §4, and the most obvious feature of the solution is the spike in β which develops for $0 \leqslant D \ll 1$. When $D = 0$, the most striking difference between the cases of quadratic autocatalysis, $n = 1$, and cubic autocatalysis, $n = 2$, occurs when the initial input of the autocatalyst, B, is discontinuous at $x = \lambda$. The spike in β then grows exponentially under cubic autocatalysis but only algebraically under quadratic autocatalysis. The most noticeable difference between the two cases for $0 < D \ll 1$ becomes apparent at $t = t_{\mathrm{II}}$ when a wave front emerges from the spike in β. Under quadratic autocatalysis this wave front immediately propagates away from the spike in β at the minimum speed, whereas under cubic autocatalysis the wave front forms within the spike in β and its propagation causes the spike to spread asymmetrically. The wave front then decelerates as $t \to t_{\mathrm{II}} = O(D^{-2})$, when it reaches the minimum propagation speed. These differences in behaviour clearly distinguish the two cases and may be observable along with the spike in β, in epidemic propagation or enzyme reactions when $0 \leqslant D_{\mathrm{B}} \ll D_{\mathrm{A}}$.

One of the authors (J. B.) acknowledges the support of a SERC Research Studentship.

Appendix

We consider here the initial/boundary value problem for $\beta_{\mathrm{II}}(X, t)$ $(|X|, t \geqslant 0)$, defined by (126*a–c*), (87*b*), with $A(t)$ defined in (86) and with asymptotic form as $t \to \infty$ given by (126*d*). We first write

$$\beta_{\mathrm{II}}(X, t) = -F(t)\zeta(X, t), \tag{A 1}$$

with $F(t)$ given by (128*d*). The initial/boundary value problem for $\zeta(X, t)$ then reduces to

$$\partial\zeta/\partial t = \partial^2\zeta/\partial X^2 - A(t)\,F(t)\zeta^2 - (F'(t)/F(t))\,\zeta, \quad t, |X| \geqslant 0, \tag{A 2}$$

$$\zeta(X, 0) = H(X) - 1 \equiv G(X), \quad |X| \geqslant 0, \tag{A 3}$$

$$\zeta \to 0 \quad \text{as} \quad X \to \infty, \quad t > 0, \tag{A 4}$$

$$\zeta \to -1 \quad \text{as} \quad X \to -\infty, \quad t > 0, \tag{A 5}$$

where $H(X)$ is the Heaviside step function. We refer to the boundary-value problem

(A 2)–(A 5) as (P1), with solution $\zeta = \zeta_e(X,t)$. Now, suppose equation (A 2) is replaced by either

$$\partial\zeta/\partial t = \partial^2\zeta/\partial X^2, \quad t, |X| \geqslant 0, \tag{A 6}$$

or

$$\partial\zeta/\partial t = -A(t)\,F(t)\zeta^2 - (F'(t)/F(t))\,\zeta, \quad t, |X| \geqslant 0, \tag{A 7}$$

with the respective modified problems labelled as (P2) and (P3). We denote the solution to (P2) as $\zeta = \zeta_D(X,t;G(\cdot))$ and that of (P3) as $\zeta = \zeta_s(t;G(X))$. The solution of (P2) is readily obtained as

$$\zeta_D(X,t;G(\cdot)) = \frac{1}{2}\int_{-\infty}^{\infty} G\left(\frac{X}{2t^{\frac{1}{2}}} - \omega\right) e^{-\omega^2}\,d\omega = -\tfrac{1}{2}\,\mathrm{erfc}\left(\frac{1}{2}\frac{X}{t^{\frac{1}{2}}}\right), \quad |X|, t \geqslant 0, \tag{A 8}$$

while the solution to (P3) is given by

$$\zeta_s(t;G(X)) = G(X)\left\{1 - \beta_0 g_\lambda \int_0^t A(\tau)\,d\tau\right\}\Big/\left\{1 + \beta_0 g_\lambda G(X)\int_0^t A(\tau)\,d\tau\right\}, \quad |X|, t \geqslant 0. \tag{A 9}$$

Note that $\zeta_s(t;G(X))$ is well-defined for all $t \geqslant 0$, via (129a) (since $A(t)$ is a monotone decreasing, positive function of $t \geqslant 0$).

We now define the functions $\zeta(X,t)$ and $\bar{\zeta}(X,t)$ to be

$$\left.\begin{aligned} \bar{\zeta}(X,t) &\equiv \zeta_s(t;\zeta_D(X,t;G(\cdot))),\\ \zeta(X,t) &\equiv \zeta_D(X,t;\zeta_s(t;G(\cdot))),\end{aligned}\right\} \quad |X|, t \geqslant 0, \tag{A 10}$$

noting that both $\bar{\zeta}$ and ζ are well defined for all $|X|, t \geqslant 0$. On using (A 8), (A 9) in (A 10) we arrive at the explicit expressions

$$\left.\begin{aligned} \zeta(X,t) &= -\tfrac{1}{2}\,\mathrm{erfc}\,(X/2t^{\frac{1}{2}}),\\ \bar{\zeta}(X,t) &= -\tfrac{1}{2}\,\mathrm{erfc}\left(\frac{X}{2t^{\frac{1}{2}}}\right)\left[1 - \beta_0 g_\lambda \int_0^t A(\tau)\,d\tau\right]\Big/\left[1 - \tfrac{1}{2}\beta_0 g_\lambda\,\mathrm{erfc}\left(\frac{X}{2t^{\frac{1}{2}}}\right)\int_0^t A(\tau)\,d\tau\right],\end{aligned}\right\} \tag{A 11}$$

for all $|X|, t \geqslant 0$. We can now establish

Theorem. *The initial/boundary-value problem* (P1) *has a unique, bounded solution* $\zeta_e(X,t)$ *on* $(X,t) \in (-\infty,\infty)\times[0,\infty)$. *Furthermore*

$$\zeta(X,t) \leqslant \zeta_e(X,t) \leqslant \bar{\zeta}(X,t) \tag{A 12}$$

for $(X,t) \in (-\infty,\infty)\times[0,\infty)$.

Proof. An application of theorem 1 of Kolodner & Pederson (1966) with

$$L[\zeta] \equiv \zeta_t - \zeta_{XX}, \quad g(t;\zeta) \equiv -A(t)\,F(t)\zeta^2 - (F'(t)/F(t))\,\zeta,$$
$$M = -1, \quad N = 0, \quad t_0 = \infty.$$

□

The inequality (128a) follows directly from (A 12), on using (A 11) and (A 1).

References

Aris, R., Gray, P. & Scott, S. K. 1988 *Chem. Engng Sci.* **43**, 207–211.

Bailey, N. J. T. 1975 *The mathematical theory of infectious diseases.* London: Griffen.

Billingham, J. 1991 Travelling waves and clock reactions in quadratic and cubic autocatalysis. Ph.D. thesis, University of East Anglia, U.K.

Billingham, J. & Needham, D. J. 1991*a* *Phil. Trans. R. Soc. Lond.* A **334**, 1–24.

Billingham, J. & Needham, D. J. 1991*b* The development of travelling waves in quadratic and cubic autocatalysis with unequal diffusion rates. III. Large time development in quadratic autocatalysis. *Q. appl. Math.* (In the press.)

Coddington, E. A. & Levinson, N. 1955 *Theory of ordinary differential equations.* New York: McGraw-Hill.

Fife, P. C. & McLeod, J. B. 1977 *Arch. ration. Mech. Analysis* **65**, 335–361.

Gray, P., Griffiths, J. F. & Scott, S. K. 1984 *Proc. R. Soc. Lond.* A **397**, 21–44.

Gray, P., Merkin, J. H., Needham, D. J. & Scott, S. K. 1990 *Proc. R. Soc. Lond.* A **430**, 509–524.

Kolodner, I. I. & Pederson, R. N. 1966 *J. diff. Equat.* **2**, 353–364.

Larson, D. A. 1978 *SIAM J. Appl. Math.* **34**, 93–103.

McKean, H. P. 1975 *Commun. pure appl. Math.* **28**, 323–331.

Merkin, J. H. & Needham, D. J. 1990 *Proc. R. Soc. Lond.* A **430**, 315–345.

Merkin, J. H., Needham, D. J. & Scott, S. K. 1985 *Proc. R. Soc. Lond.* A **398**, 81–116.

Merkin, J. H., Needham, D. J. & Scott, S. K. 1989 *Proc. R. Soc. Lond.* A **424**, 187–209.

Sel'kov, E. E. 1968 *Euro. J. Biochem.* **4**, 79–86.

Stewartson, K. 1957 *J. Math. Phys.* **36**, 173–191.

Van Dyke, M. 1975 *Perturbation methods in fluid mechanics.* Stanford: Parabolic Press.

Watson, E. J. 1981 *Laplace transforms and applications.* Van Norstrand, Reinhold.

Received 10 December 1990; accepted 26 February 1991

PHILOSOPHICAL TRANSACTIONS OF THE ROYAL SOCIETY A MATHEMATICAL, PHYSICAL & ENGINEERING SCIENCES